



EML 4905 Senior Design Project

A B.S. THESIS

PREPARED IN PARTIAL FULFILLMENT OF THE
REQUIREMENT FOR THE DEGREE OF
BACHELOR OF SCIENCE IN MECHANICAL ENGINEERING

**POWER-GENERATING
WIND MITIGATION DEVICE**

100% Report

Marcos A. Balmaseda

Yoel Tanquero

Yunior Licea

Advisor: Professor Andrés Tremante

April 3rd, 2014

This B.S. thesis is written in partial fulfillment of the requirements in EML 4905. The contents represent the opinion of the authors and not the Department of Mechanical and Materials Engineering.

Ethics Statement and Signatures

The work submitted in this B.S. thesis is solely prepared by a team consisting of Marcos A. Balmaseda, Yoel Tanquero, and Yunion Licea and it is original. Excerpts from others' work have been clearly identified, their work acknowledged within the text and listed in the list of references. All of the engineering drawings, computer programs, formulations, design work, prototype development, and testing reported in this document are also original and prepared by the same team of students.

Marcos A. Balmaseda Team Leader	Yoel Tanquero Team Member	Yunion Licea Team Member
---------------------------------------	------------------------------	-----------------------------

Dr. Andrés Tremante
Faculty Advisor

ABSTRACT

This project proposes the development of a horizontal wind turbine to be installed at the edge of the roof of a house or similar structure. The purpose of this device is to mitigate the effects of the pressure gradient produced by the flow of air over a roof at elevated speeds during a hurricane. Furthermore, this proposed design produces electricity by harvesting the kinetic energy carried by the fluid during the hurricane as well as under normal weather conditions.

The design phase of this revolutionary device considers variables such as diameter to length ratio, number of blades, shape of the blades, angle of twist, material used for prototype construction, and optimal location of the device relative to the structure's roof. Computational Fluid Dynamic (CFD) studies are performed on the proposed design to investigate the viability of this system. In addition, an estimated power generation capacity of the model is assessed with the obtained pressure readings. After the CFD study is concluded, experimental trials of the turbine model are conducted in Florida International University's Wall of Wind to validate the results of this analysis.

DEDICATION

First and foremost, I dedicate this thesis to the living God “Elohim Chayim.” I also dedicate this senior design project to my family. I will constantly be grateful for all their support and kindness through my life-time. Special appreciation to my lovely wife; Yilian Pineda has been by my side through this journey. My parents and brother, Ricardo Licea, Amarilis Rosales and David Licea, whose words of perseverance and encouragement pushed me to reach this goal and become a better person.

Yunior Licea

I dedicate this paper to all family and friends that are always there for me when I need them the most. Special thanks to our advisors.

Yoel Tanquero

To my family and friends, for their unconditional support to my education and success.
Thank you.

Marcos Ahmed Balmaseda

ACKNOWLEDGEMENTS

We would like to thank our advisors Dr. Andres Tremante and Mr. Javier Palencia, who were very generous with their expertise and valuable time. Special thanks to P.E. Pelayo Calante for his unconditional guidance and dedication through this process. We would like to express our gratitude to Dr. Igor Tsukanov, Dr. Seckin Gokaltun for their assistance with ANSYS. Additionally, we wish to acknowledge Mr. Rick Zicarelli for his support. Also, we would like to thank Ms. Rocio Hernandez for providing any assistance requested. Finally, special thanks to Paola Davalos and Sergio Baltodano for their valuable contributions to this project.

Contents

1.	INTRODUCTION.....	10
1.1	Problem Statement.....	12
1.2	Motivation.....	13
1.3	Literature Survey	14
1.3.1	Characteristics of Winds during a Hurricane	14
1.3.2	Previous Wind Mitigation Devices.....	16
1.3.3	Types of Wind Turbines Available	16
1.3.4	Wind Turbines for Energy Production	21
1.3.5	Electric Generators	22
1.3.6	Wind Turbine for Hurricane Wind Mitigation	23
1.3.7	LEED Certification.....	24
2.	PROJECT OBJECTIVES	26
3.	ANALYTICAL CONSIDERATIONS	27
3.1	Wind Energy.....	27
3.2	Ideal Wind Turbine.....	28
3.3	Savonius Wind Turbine	32
3.4	Boundary Layer Effect.....	34
3.5	Flow Separation	38
3.6	Flow pattern around a cylinder	39
3.7	Flow pattern around rotating cylinder.....	42
3.7.1	Rotating cylinder with axial flow	42
3.7.2	Rotating cylinder with normal flow.....	44

3.8	Dimensional Analysis	45
4.	FIRST PROTOTYPE.....	48
4.1	Prototype System Description.....	48
4.2	Experimental Testing and Results	49
5.	DESIGN STUDY.....	51
5.1	Initial Analysis: Using Straight Blade Turbine.....	53
5.1.1	Initial Mesh Study	54
5.1.2	Finding Best Number of Blades, Using Improved Geometry and Mesh 65	
5.1.3	Finding X and Y Position of the Turbine in Relation to the Roof of the House 69	
5.2	Computational VS Experimental Results: Progression Study	71
5.2.1	Initial Experimental Setup.....	72
5.2.2	House.....	79
5.2.3	Straight Blade	80
5.2.4	Straight Blade Twisted	82
5.2.5	Two Blade Savonius.....	84
5.2.6	Three and Four Blade Savonius.....	86
5.2.7	Discussion.....	89
5.3	Proposed Design	90
6.	ESTIMATIONS FOR PROTOTYPE	92
6.1	Dimensionless analysis for power generation.....	93
6.2	Other Considerations: Electrical Setup.....	97
6.2.1	Electrical Setup Alternative 1: House Grid Connected System	100

6.2.2	Electrical Setup Alternative 2: House Grid Connected System with Storage	100
6.2.3	Electrical Setup Alternative 3: Power Provider Grid-Connected System	101
6.2.4	Feasibility Assessment	101
7.	COST ANALYSIS	102
7.1	First Prototype.....	102
7.2	Experiment Parts and Equipment.....	103
7.3	Prototype	103
7.4	Electrical System for Prototype	104
8.	TIMELINE AND RESPONSIBILITIES	105
9.	CONCLUSIONS	106
10.	RECOMMENDATIONS.....	108
11.	REFERENCES	112
12.	APPENDIX	115
12.1	Appendix A: Engineering Drawings.....	115

List of Figures

Figure 1. Wind behavior over a roof.....	15
Figure 2. Wind corner vortices over a roof.....	15
Figure 3: HAWT wind farm	17
Figure 4. VAWT, Savonius	19
Figure 5. VAWT, Darrieus	19
Figure 6. Double-blade Savonius.....	20
Figure 7: Windside turbine	20
Figure 8. HAWT and VAWT schematic	22
Figure 9. Idealized wind turbine and stream-tube analysis of flow (White, 2001)	29
Figure 10. Estimated performance of various wind turbine designs as a function of blade-tip speed ratio. (Ragheb, 2011)	31
Figure 11. Boundary Layer growth in a flat plate (White, 2001)	35
Figure 12. Boundary layer on a flat plate (vertical thickness exaggerated greatly. (Pritchard, 2011)	37
Figure 13. Kármán vortex street (ESPEYRAC & PASCAUD)	39
Figure 14. Separation in a sphere immerse in (a) laminar flow (b) turbulent flow (White, 2001)	40
Figure 15. Boundary layer flow over a rotating cylinder with superposed axial flow. (Childs, 2011)	42
Figure 16. Flow pattern (a) through a cylinder, (b) due to rotation, (c) combination of patterns (Childs, 2011).....	44

Figure 17. Lift and drag coefficients for a smooth spinning sphere in a uniform flow (Childs, 2011)	45
Figure 18: First built prototype	48
Figure 19. (a) horizontal (b) 45 degree (c) 90 degree	49
Figure 20. (a) experiment without device (b) experiment with device	50
Figure 21. Corner winds prototype test.....	50
Figure 22: Analysis progression. (a) House alone. (b) House with straight blade turbine. (c) House with twisted straight blade turbine. (d) House with twisted 2-blade Savonius turbine. (e) House with twisted 3-blade Savonius turbine. (f) House with twisted 4-blade Savonius turbine	51
Figure 23: 2D wind turbine front view	54
Figure 24: Study geometry with house	65
Figure 25: Improved geometry and mesh for initial study	66
Figure 26: Pressure over the roof of the house for improved geometry and mesh study	68
Figure 27. Pressure profiles for different X positions.....	70
Figure 28. Pressure profiles for different Y positions.....	71
Figure 29. Velocity profiles in the wind tunnel	72
Figure 30: 2D cross-sectional area of the wind tunnel	73
Figure 31. Velocity airflow-meter vs. Pitot-tube	74
Figure 32: 3D-printed house roof	76
Figure 33: Roughness surface lecture	76

Figure 34: Roof setup for pressure reading.....	77
Figure 35: Data acquisition unit setup for pressure reading	77
Figure 36. LINI-T 5URH0 digital tachometer	78
Figure 37. Three straight blades turbine, experimental setup.....	79
Figure 38. Static pressure house at 8m/s.....	80
Figure 39. Static pressure house at 10m/s.....	80
Figure 40. Static pressure 3 blades straight at 8m/s.....	81
Figure 41. Static pressure 3 blades straight at 10m/s.....	81
Figure 42. Static pressure 3 blades twisted at 8m/s	83
Figure 43. Static pressure 3 blades twisted at 10m/s	83
Figure 44. Two-blades Savonius turbine	85
Figure 45. Static pressure 2 blades Savonius at 8m/s	85
Figure 46. Static pressure 2 blades Savonius at 10m/s	86
Figure 47. Static pressure 3 blades Savonius at 8m/s	87
Figure 48. Static pressure 3 blades Savonius at 10m/s	87
Figure 49. Static pressure 4 blades Savonius at 8m/s	88
Figure 50. Static pressure 4 blades Savonius at 10m/s	88
Figure 51: 3D printed roof, pattern of the layers	90
Figure 52: Pressure profile over roof for 8 m/s velocity.....	91
Figure 53: Pressure profile over roof for 10 m/s velocity.....	91
Figure 54: Electrical setup alternative 1	100
Figure 55: Electrical setup alternative 2	100

Figure 56: Electrical setup alternative 3	101
Figure 57: Timeline.....	105
Figure 58. Team responsibilities.....	106

List of Tables

Table 1. Drag coefficient data for selected objects ($Re > 10^3$).....	41
Table 2. Design parameters for prototype calculations	54
Table 3: Boundary layer thickness calculations.....	68
Table 4. X and Y offset positions	69
Table 5. Angular speed of 3 blades with and without an angle of twist.	84
Table 6: Angular speed of 2, 3 and 4 blades Savonius.	89
Table 7: Experimental angular velocity at different wind speeds for 3-blade Savonius model.....	94
Table 8: Angular velocity at different wind speeds for 3-blade Savonius real-size turbine	96
Table 9: Torque and power calculations for prototype.....	96
Table 10. Prototype cost analysis.....	103
Table 11: Cost of experimental parts and equipment	103
12: Estimated cost of prototype	104

NOMENCLATURE

Symbol	Description	Unit
P	Power	W
t	Time/Thickness of blade	s/m
m	Mass	kg
\dot{m}	Mass flow rate	kg/s
V	Velocity	m/s
ρ	Density	kg/m ³
A	Area	m ²
F	Force	N
p	Pressure	Pa
C_p	Coefficient of power	-
C_t	Coefficient of Torque	-
ω, Ω	Angular velocity	rad/s
d, D	Diameter	m
T	Torque	N-m
I	Moment of Inertia	m ⁴
α	Angular acceleration	rad/s ²
l	Length	m
r, a	Radius	m

θ	Angle of attack	rad
h	Height	m
U, u	Horizontal velocity	m/s
δ	Boundary layer thickness	m
τ	Shear force	N/m ²
C_f	Skin friction coefficient	-
Re	Reynolds number	-
μ	Viscosity	kg/(m·s)
C_D	Drag coefficient	-
C_L	Lift coefficient	-
λ	Rotation parameter	-
M	Mach Number	-
c	Speed of sound	m/s

1. INTRODUCTION

Hurricane season represents a very important natural phenomenon for several regions worldwide, in particular to South Florida and its neighboring areas. Hurricanes come accompanied by severe rain as well as very strong winds. The destructive force of these winds is very high, especially for houses built using traditional construction methods. There is an imperative need for engineering solutions to improve the resistance of common houses to withstand the devastating forces of winds produced by a hurricane. Florida and the neighboring Caribbean countries are faced with the destructive and possibly fatal catastrophes caused by these natural disasters without innovative hurricane mitigation research and implementation.

Disasters produced by the devastating action of a hurricane's powerful winds often involve high economic losses mainly due to buildings' roofs lifting under the force of suction of the air. The tremendous pressure difference between the upstream and downstream conditions of the flow of air during a hurricane causes the lifting force that detaches the roof from the rest of the structure. This is known as the "Uplift Effect."

Another very important aspect to consider is the energy crisis that the world is going through nowadays. The planet's limited natural resources are being exploited more than ever. To illustrate, according to the Hirsch Report published by the Department of Energy of the U.S. in 2005, it is expected that the world will reach oil production peak within the next 15 to 20 years (Hirsch, Bezdek, & Wendling, 2005). This means that more pollution is being released into the atmosphere, and this pollution is destroying the Earth's natural defenses such as the Ozone Layer. A clean alternative to reduce the exploitation of these

fossil fuels is the development of technologies that use renewable sources such as wind and sunlight to generate green energy. According to the article published by ExxonMobil “*The Outlook for Energy, A view to 2040*,” it is expected that wind and solar will contribute to about 10% of electricity generation in 2040; that represents 9 percent increase from the 1% contribution in 2010. Thus, wind and solar energy have a very large potential that is still to be exploited.

Wind energy is an inexhaustible and renewable source available almost anywhere on the planet. Wind is usually generated by the difference in temperature across the globe and other geographical features. This energy has been used for thousands of years and it has played an incredible role in the development of the human kind. The most common example is the four-bladed windmill which during centuries allowed the pumping of water, grinding of grain and the sawing of woods in countries like Holland, England and Greece. Additionally, the use of wind energy in watercrafts allowed the commerce and even the discovery of America in 1492.

This energy differentiates from other sources in many aspects: it’s renewable, abundant, the technology needed is available today, and does not require huge areas for its extraction. It is for that reason that more and more studies are being conducted today in order to better use this renewable source.

A very innovative and effective way to address both problems explained above is to create a device that has a double purpose. The first purpose is to mitigate the force of the winds during a hurricane; and the second purpose is to generate clean electricity by harvesting the energy carried by the wind.

After the successful completion of this project, structures that incorporate the design proposed would be able to withstand stronger forces and survive the passing of hurricanes. Furthermore, the possessor of such device would be able to generate and use clean energy while contributing to the protection and conservation of our planet Earth.

1.1 Problem Statement

There is a need for innovative engineering solutions to mitigate the destruction caused by hurricanes. The uplift effect caused by the flow separation over the roof of a house is the main reason for roofs flying off during a hurricane. Thousands of homeowners lose their homes every year with the passing of major storms. After hurricane Andrew, Florida authorities and other entities started the investigation and development of new technologies with the objective of preventing and reducing the destruction caused by such natural disasters.

Furthermore, power generation is extinguishing the planet's limited resources. Issues like CO₂ emissions and global warming need to be addressed. For that reason, developments of new technologies to generate electricity using inexhaustible green energy sources is of paramount importance for the immediate future.

This project aims at solving both problems by creating an innovative device that mitigates the uplift effect during a hurricane; and harvests the kinetic energy of the wind to generate clean electricity. Thus, a system that allows the solution of both issues at the same time should have a significant impact on the area.

1.2 Motivation

The State of Florida, like most of the Caribbean countries, has always been under the scope of hurricanes. The geographic location of the sunshine state places it in a dangerous position during hurricane season. The losses and damages that Floridian houses have suffered under the actions of windstorms represent the driving motive for engineers and contractors to look for ways and alternatives to improve the strength and safety of houses. Nothing can be done to stop natural forces from happening; however, it is possible to work towards our preservation, comfort, and security by improving aspects of life such as structural strength and safety of houses.

Economic sustainability is another reason to find new strengths and improvements in the field of wind and extreme weather mitigation. Hurricane disasters are the cause of significant economic losses in the Southeast region of the United States, especially in Florida, as well as in the Caribbean and some regions of South America every year. Major hurricanes such as Andrew, Ivan, Katrina and Wilma, have impacted Florida causing severe physical and economical losses. It is estimated that these losses will continue to increase as the population grows in the coastal areas. For that reason, it is necessary to improve engineering methods and practices to protect Floridian's homes and also Floridian's lives. As a result of improved engineering techniques to protect against climate contingencies, financial and social costs could be decreased when facing hurricane activity.

One of the primary concerns during a hurricane is the damage caused by the strong winds. Research shows that the roof of a house is very vulnerable due to large pressure differences produced by winds. For that reason, this team decided to help diminish the

losses resulting from a hurricane by building a turbine that can be installed in any house to serve as a wind mitigation device.

Finally, there is another concern that has become increasingly important for humankind in the last few years: the burning of fossil fuels for electricity production. This is a very delicate situation because all the pollution produced is one of the main factors causing global warming and destroying the ozone layer. For that reason, there is an imperative need to find new sources of energy to use for electric power production. There is much research being done to find renewable sources such as water and wind to produce electricity; and these clean forms of energy are expected to eventually replace the traditional fuel burning methods today. Thus, the model proposed in this project is intended to be implemented nation and worldwide because it also provides a way to take advantage of wind energy under normal weather conditions and use it as a renewable and clean source to produce energy.

1.3 Literature Survey

1.3.1 Characteristics of Winds during a Hurricane

The force created by the wind during a hurricane generally produces significant damage. According to the National Hurricane Center, a category 5 hurricane is accompanied by winds with speeds of 150 miles per hour (about 67 m/s) or higher, which most likely causes catastrophic damage to structures. This damage generally starts as a failure of the roof, and following destruction of the rest of the structure including walls and interiors.

One characteristic of hurricane winds that also contributes to the lifting of the roofs and destruction of the structures is the fluctuation of the flow field. If the speed and patterns of the flow were constant, it would be easier for the engineers to design a structure capable of enduring these forces. However, changing conditions produce fatigue in the different supporting elements that ultimately cause failure.

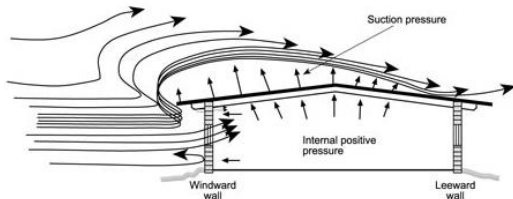


Figure 1. Wind behavior over a roof

Another characteristic of hurricane winds is the turbulence that accompanies the flow of wind. Turbulent flows carry much more energy than laminar flows, and this energy can be transferred into the structure causing the failure (Manwell.)

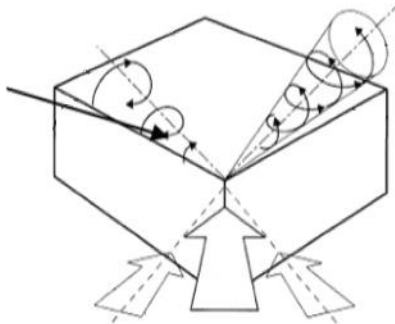


Figure 2. Wind corner vortices over a roof

The main concern of this project is the uplift effect caused by the strong winds. Figure 1. Wind behavior over a roof shows what happens on the roof of a house when strong winds are acting upon it. The empty space that

forms between the layers of air and the surface of the roof causes a vacuum effect that produces the uplift and ultimately the failure of the roof. Another risk presented by high hurricane winds happens when the direction of the wind is at an angle with the roof. Figure 2. Wind corner vortices over a roof shows the conical vortices formed when winds strike the house in the corners. These vortices increase the pressure difference that causes lift and produces a greater uplift effect (Lin 2008.)

1.3.2 Previous Wind Mitigation Devices

There has been extensive research dedicated to the development of mitigation alternatives that can be easily retrofitted into existing structures. AEROEDGE™ Vortex Suppression Technology is an example of these kinds of mitigation devices. This technology was developed by RenaissanceRe group and tested in the 6-fan Wall of Wind at Florida International University. This technology has proven effective in the reduction of the pressure gradient on roofs during high winds, and experimental results confirm this (Lin 2008.) These types of static devices have been studied and improved over the years, with the aforementioned being one of the latest developments.

While research has found different sorts of static devices to fight wind, the model proposed in this project is a completely new approach that has rarely been studied before. The wind turbine developed in this thesis is a new kind of dynamic device that has a dual purpose; it mitigates the force of strong winds while generating clean energy.

1.3.3 Types of Wind Turbines Available

Wind turbines are devices that convert the kinetic energy of the wind into useful energy that can be harvested such as mechanical energy. The main idea behind the basic operation of wind turbines is to use the force of the wind to rotate the blades. This way, the energy carried by the wind can be turned into mechanical energy, which can then be used to generate and store electrical energy. In modern wind turbines, the basic principle of lift produced by the wind is used to rotate the blades of the turbine and produce the torque necessary to move a shaft (Manwell, McGowan, & Rogers, 2009). There are two main

kinds of wind turbines: horizontal and vertical axis. Following is a brief description of them.

Horizontal Axis Wind Turbines (HAWT)

These are the most commonly used wind turbines worldwide. Some of the leading manufacturers include General Electric, Vestas, Urban Green Energy, and Northern Power



Figure 3: HAWT wind farm

Systems. The main characteristic of these kinds of turbines is that their axis of rotation is parallel to the ground as shown in **Error! Reference source not found..**

A HAWT consists of different parts such as the rotor and drive train.

The rotor of a HAWT includes the blades and supporting hub of the device. The blades are the heart of a wind turbine because they are the elements directly interacting with the wind. These kinds of turbines use aerodynamically designed blades to take advantage of the forces generated by the wind. These blades, usually three of them, must be facing the wind according to their design specifications. In other words, the blades must be oriented perpendicular to the direction of the wind. It is because of this requirement that all HAWT must have a device to rotate them and orient them correctly as the wind changes its direction. Usually these directional correctors are in the form of a wind-vane for small turbines, while larger turbines use electronic devices and sensors to correct directional changes. Moreover, these blades are usually made of very light weight materials to

facilitate transportation and installation as well as to increase efficiency in harvesting energy from the wind (Paraschivoiu, 2009).

The drive train of a HAWT consists of other rotating parts and components such as gears, bearings, and couplings. One of the main mechanisms of this drive train is the gearbox. The main function of this gearbox is to increase the velocity of rotation of the blades and transmit this power down through the shaft to the system that ultimately converts this rotational energy into useful electrical energy. It is very important to increase the rotational speed provided to the electric generator because the power generated by these machines is usually a function directly proportional to the speed of rotation of the shaft; therefore, the faster the shaft is rotating, the more electricity can be generated. However, there is an ideal value for this increase in speed that can be calculated because it is important to take into consideration the losses with each transformation. In summary, the perfect balance between rotational speed of the blades and output rotational speed of the shaft must be found in order to design the optimal gearbox and obtain the maximum possible efficiency from the wind turbine.

Vertical Axis Wind Turbines (VAWT)



Figure 4. VAWT, Savonius



Figure 5. VAWT, Darrieus

These kinds of wind turbines were studied extensively in the 1970s and 1980s particularly in the U.S. and Canada. The most important characteristic of these types of turbines is that they can accept wind coming from any direction, which is very advantageous and helps simplify the design and complexity of the mechanism. These kinds of turbine, like the HAWT, are composed of a rotor and a drivetrain.

The rotor of a VAWT serves the same purpose as the other kind of turbine explained before; the main difference here is that the blades generally have a shape that allows them to accept winds coming from any direction.

The drivetrain of a VAWT is similar to that of a HAWT; the only difference is that the shaft connected to the rotor is vertical instead of horizontal. In addition, the same gearbox idea must be used here for the same purpose.

Common examples of these vertical-axis wind turbines are the Savonius Rotor (Figure 4. VAWT, Savonius) and Darrieus turbines (Figure 5. VAWT, Darrieus) (Paraschivoiu, 2009).

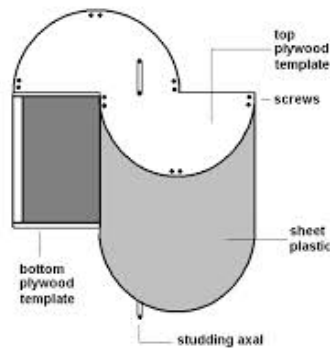


Figure 6. Double-blade Savonius

Savonius wind turbines have a characteristic cross sectional area as shown in Figure 6. Double-blade Savonius. These kinds of turbines may have two or more blades. Also, they can have a different configuration from the one shown; in some models the semi-cylinders do not cross each other in the center section. However, the most commonly seen Savonius turbines are similar to those shown in Figure 6. Double-blade Savonius, in which there is a space between the two “blades”

that allows air to circulate.

Darrieus wind turbines are another kind of vertical axis wind turbines commonly seen nowadays. The first patent of this type of device was awarded in 1931 to the French engineer G.J.M. Darrieus by the U.S. Patent Office (Paraschivoiu, 2009). These types of wind turbines are composed of curved blades mounted on a vertical axis that can accept winds coming from any direction as well.



Figure 7: Windside turbine

Finally, Oy Windside Production Ltd. is a Finland-based company that has developed a vertical axis wind turbine with generation capabilities close to the horizontal axis wind turbines.

The Windside turbines range from 0.15 square meters of area to 12 square meters, and their average annual generation capabilities range from 40 kWh to 8640 kWh. Additionally, the company claims that “select models are guaranteed to: 20m/s, 30m/s, 40m/s, 50m/s, and 60m/s (216Km/hour).” (Oy Windside Production Ltd)

The turbines are composed of different materials. The vanes are made of fiber glass, the fastenings are aluminum, the shaft is chrome coated steel, and all the bolts are stainless steel. It is clear that the objective is to maintain a structural strength while reducing the weight.

In Summary, wind turbines have been used for years to generate electrical power. Although there are many patents that have improved on the initial designs, the HAWT and VAWT are the most commonly used wind turbines nowadays.

1.3.4 Wind Turbines for Energy Production

The primary function of wind turbines nowadays is the production of electric power. There have been many efforts around the world to promote the use of renewable sources of energy, such as the wind, to produce electricity. In the United States, for example, the American Recovery and Re-investment Act of 2009 provides tax cuts to renewable energy decisions. Installed Wind Turbines qualify for up to 30% federal tax credit, which contributes to further develop and improve the existing designs and to encourage enterprises to implement these types of energy source.

Research efforts internationally have contributed to the development of new technologies that take advantage of this renewable source of “free” energy. According to information published by the National Renewable Energy Laboratory in its January 2012 Energy Update, the world’s total installed wind capacity increased from 50,000 MW in 2005 to around 216,000MW in 2012. The leading countries taking advantage of this renewable source are China, the U.S., Germany, Spain, and India. These facts clearly show a trace that can be easily interpreted as a new era in which a much cleaner energy is the main component.

On the other hand, even when there have been significant improvements in electricity generation utilizing wind power, most of this generation comes from wind farms. However, there

is not much advancement shown at the smaller scale. In other words, not much of the improvements and new technologies implemented in the last few years can be used by individuals to be installed in the houses and small constructions all over the country. For that reason, there is a wide field of research and exploration to be exploited, and this project is aimed at taking the first steps towards this initiative.

1.3.5 Electric Generators

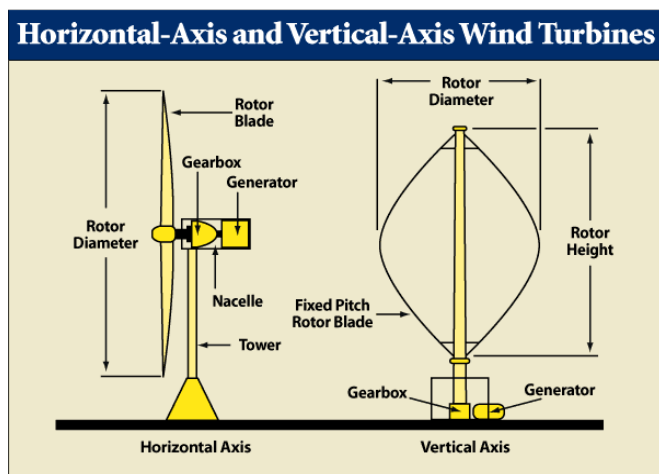


Figure 8. HAWT and VAWT schematic

The generation of electric energy on a horizontal axis wind turbine with a rotor diameter of up to 120 meters is up to 5 MW (Woodbank). The turbine is controlled to maintain a constant angular velocity for any wind speed. The angular velocity of the blades is in the range of 10 to 20 RPM. The rotor transmits the torque to a gear box that controls the number of RPM to a fix value,

depending of the country to be installed. Usually, this value is 1200 RPM so that the frequency of the AC current is 60 Hz, which what is used in the United States.

For vertical axis wind turbines, the generation of energy occurs in a similar way. The main difference is that vertical axis wind turbines are mostly for domestic small installations; therefore, the cost of the turbine is reduced by eliminating the speed controller that keeps the angular velocity

of the rotor constant¹. As a result, the frequency and amount of current produced changes with the changes in wind speed. Then, the current produced by the turbine is adjusted and stored by a separate device. Subsequently, the energy stored can be used for different applications.

1.3.6 Wind Turbine for Hurricane Wind Mitigation

A great amount of information is available about the behavior of the winds during a hurricane. There are many articles explaining how hurricane winds impact different buildings and structures with different shapes. For example, the American Society of Civil Engineers (ASCE) Online Library contains several articles that analyze and characterize hurricane winds. Furthermore, researchers talk about the importance of improving the construction standards to make structures more resistant to wind forces produced by high speed winds. One example of the improvements that have been taking place in the last few years is the modifications that the Florida Building Code have experienced in the aftermath years of hurricanes Katrina and Wilma in 2005. A good example of these improvements is explained and visualized in a video recorded the inaugural day of the Wall of Wind Laboratory at the Florida International University (FIU). This video can be found in the website of the International Hurricane Research Center of FIU. The video shows two small houses, one built to the standards before these major hurricanes, and the other one built to the new improved standards. When these two houses are placed in a hurricane strength wind scenario, it is clearly seen the one built following the new code was more resistant.

Nevertheless, there is no indication of a device similar to the one proposed in this project that serves to mitigate the force of the winds during a hurricane. For that reason, this project can

¹ * Source: “*Window on State Government*” website

serve as the initial steps towards a new era of hurricane mitigation devices that can also be used for other purposes such as energy generation using renewable sources.

1.3.7 LEED Certification

Leadership in Energy and Environmental Design (LEED) is a system created in 1998 by the United States Green Building Council (USGBC). This system promotes the use of renewable sources in the creation, establishment, development, function, and preservation of green constructions. LEED also covers all elements of building construction such as water, energy, materials, site, design innovation and air quality. The importance of LEED lies on the impact of environmental consciousness to create sustainable products that enhance the environment. LEED is gaining popularity among companies, manufacturers and designers that are being challenged to use renewable sources to create better and more competitive products with greater recyclable potential. An entity that supports a green image and complies with the LEED standards shows its commitment to life preservation.

In order to be LEED certified it is important to know how credits relate to each other and how their combination affects a specific project. The rating system of LEED consists of four levels guided by points. According to LEED Reference Guide for Green Building Design and Construction, 40-49 points provide a rating of Certified; 50-59 points is a Silver rating; 60-79 points is a Gold, and 80 points and above means Platinum. These points are related to five categories for green design. These categories are: sustainable sites, water efficiency, energy and atmosphere, materials and resources, and indoor environmental quality. The applicant project is rated in relation to the degree of adherence within the rating system.

Since the design proposed in this project aims to use renewable energy for power generation, it is intended to comply with LEED Green Building Rating System. One of the categories mentioned above that applies to the proposed design is Energy and Atmosphere (EA) which refers as Credit #2 On-Site Renewable Energy in the Green Building Design and Construction handbook. This credit ranges between 1-7 points. It is essential to mention that the goal of the On-Site Renewable Energy is to motivate and identify growing magnitude of on-site renewable energy as a way to minimize the use of fossil fuel energy. Similarly, the proposed device uses the wind energy on a daily basis to generate electric power; hence, it meets the above requirement. Additionally, as stated by Green Building Design and Construction handbook, “Wind Powering in America is an initiative by the U.S. Department of Energy to dramatically increase the use of wind energy in the United States.” One reason for using renewable energy is that it has favorable environmental and economic impact. Another reason is the fact that on-site renewable energy applied science could be cost-effective. Actually, there are some utility discounts to encourage those who first invest in renewable energy appliances.

Another category that applies to the proposed device is Innovation in Design (ID), which refers as Credit #1 Innovation in Design in the Green Building Design and Construction handbook. This credit ranges between 1-5 points. The main goal of this category is to encourage teams to develop new designs that fulfill LEED’s guidelines. Additionally, based on Green Building Design and Construction handbook, “Only innovative strategies that demonstrate a comprehensive approach and have significant, measurable environmental benefits are applicable.” Furthermore, the proposed horizontal wind turbine is used to mitigate winds during a hurricane season, but in a different way. It is placed on the edge of the building's roof in order to reduce the uplift effect

caused by the heavy winds. This new approach of wind mitigation aims towards the Innovation in Design category mentioned above. Moreover, the suggested device is considered a new detailed method that has a tremendous impact not only environmentally, but also economically.

2. PROJECT OBJECTIVES

The main objective pursuit on this paper is the design of a device that generates electric power as well as mitigates the uplift effect generated by strong winds. The device itself follows a new concept of dynamic wind mitigation.

The uplift effect in essence is generated by the flow separation that occurs in the roof of the houses. In common passive mitigation devices, air is smoothly redirected over the roof of the houses; therefore, the wind is never in contact with the roof and separation never occurs. This new concept pursues the generation of controlled turbulent flow after the device; thus reducing or eliminating the separation vortices and uplift effect. Besides being a new and revolutionary concept on wind mitigation, this project plans the design of a device similar to a wind turbine that generates electric power with low wind speed throughout the entire year. The power generation follows the precedents established by horizontal and vertical axis wind turbines.

Although this paper does not discuss all the details related to the implementation of the device, it was developed taking into consideration the most important aspects of design and implementation.

3. ANALYTICAL CONSIDERATIONS

3.1 Wind Energy

The wind is a mass of air in movement; therefore, the kinetic energy of the wind can be defined as:

$$E_{kinetic} = \frac{1}{2} * m_{air} * V^2$$

Where,

$E_{kinetic}$: Kinetic energy of the wind [J]

m_{air} : Mass of air [Kg]

V : Wind velocity [m/s]

Power is defined as the amount of energy consumed per unit time; hence, the power of the wind can be defined as:

$$P = \frac{dE_{kinetic}}{dt}$$

$$P = \frac{1}{2} * \frac{dm_{air}}{dt} * V^2$$

Where,

P : Power of the wind [W]

The mass flow rate of air is equal to the mass of air that passes through a given area in a given amount of time; therefore, it can be expressed as:

$$\frac{dm_{air}}{dt} = \dot{m} = \rho AV_1$$

Where,

\dot{m} : Mass flow rate

ρ : Density of Air

A : Area

V : Wind Speed

As a result, the wind stream power through A is given by:

$$P_{Air} = \frac{1}{2} \rho AV_1^3$$

3.2 Ideal Wind Turbine

The ideal wind turbine, predicted by A. Betz in 1920, used a configuration similar to that one shown in Figure 9. Idealized wind turbine and stream-tube analysis of flow.

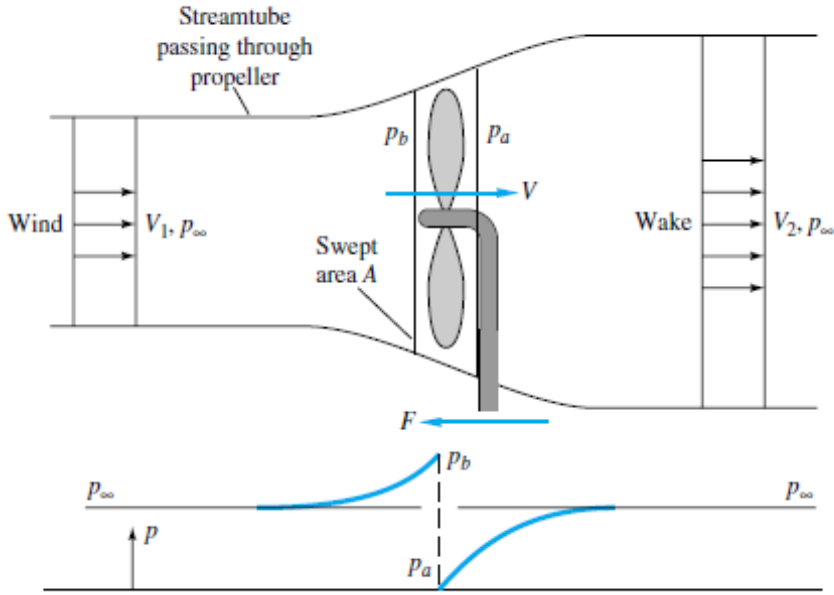


Figure 9. Idealized wind turbine and stream-tube analysis of flow (White, 2001)

The propeller creates a discontinuity of area A and local velocity V . It is clear that $V_1 > V_2$ for the wind. It is also appreciable how the pressure rises to p_b just before the turbine and drops exactly after to p_a , returning to the initial pressure as it gets far from the turbine. Moreover, this pressure is compensated by a reaction force F in an opposite direction to the flow. It then can be established that,

$$\sum F_x = 0$$

$$F = (p_b - p_a)A = \dot{m}(V_1 - V_2)$$

Assuming that the flow is ideal, the pressures can be found for each section by using the Bernoulli relation,

$$\text{From 1 to b: } p_\infty + \frac{1}{2}\rho V_1^2 = p_b + \frac{1}{2}\rho V^2$$

$$\text{From a to 2: } p_a + \frac{1}{2}\rho V^2 = p_\infty + \frac{1}{2}\rho V_2^2$$

Combining these two equations we have,

$$V = \frac{1}{2}(V_1 + V_2)$$

Hence, the velocity required through the turbine has to be equal to the average of the wind and far-wake speeds. The power extracted by the turbine can be written in terms of V_1 and V_2 as follows,

$$P_{Air} = \rho AV^2(V_1 - V_2) = \frac{1}{4}\rho A(V_1^2 - V_2^2)(V_1 + V_2)$$

By assuming a given value for V_1 and differentiating P with respect to V_2 we obtain,

$$P = P_{max} = \frac{8}{27}\rho AV_1^3 \quad \text{at} \quad V_2 = \frac{1}{3}V_1$$

Hence,

$$V = \frac{2V_1}{3}$$

While the power available is equal to,

$$P_{available} = \frac{1}{2}\dot{m}V_1^2 = \frac{1}{2}\rho AV_1^3$$

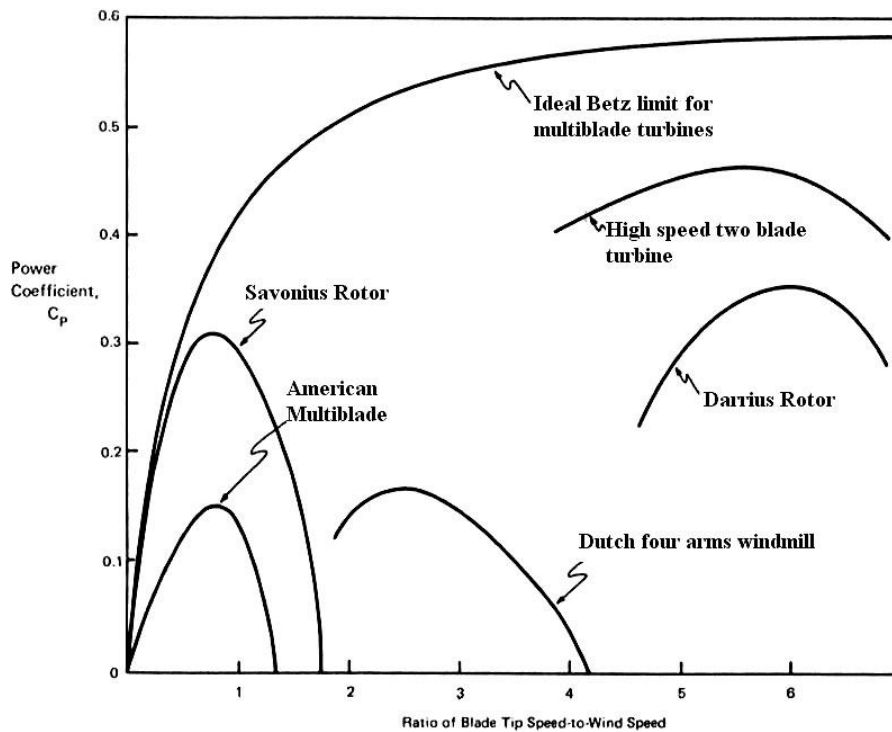


Figure 10. Estimated performance of various wind turbine designs as a function of blade-tip speed ratio. (Ragheb, 2011)

Therefore, the maximum possible efficiency of an ideal frictionless wind turbine is equal to,

$$C_p = \frac{P}{\frac{1}{2} \rho A V_1^3}$$

$$C_{p,max} = \frac{16}{27} = 0.593$$

This last number is called the Betz number and it defines the maximum ideal efficiency value for a turbine. It can be appreciated from Figure 10. Estimated performance of various wind turbine designs as a function of blade-tip speed ratio. that all other wind turbines are usually compared to this Betz value.

3.3 Savonius Wind Turbine

In his article “Experimental Comparison Study for Savonius Wind Turbine of Two & Three Blades at Low Wind Speed”, Ali discusses how three basic rules define the Savonius wind turbine performance.

- 1- The speed of the blade tips is ideally proportional to the speed of wind.
- 2- The maximum torque is proportional to the speed of wind squared.
- 3- The maximum power is proportional to the speed of wind cubed.

The performance of a wind turbine is defined by three important coefficients. Those coefficients are, the torque coefficient (C_t), the coefficient of power (C_p), and the tip speed ratio (TSR). The tip speed ratio is defined by the following equation.

$$TSR = \frac{V_{rotor}}{V_{air}}$$

Since the velocity of the rotor correspond to the velocity on the tip of the Savonius blade, this tangential velocity can be expressed in terms of the angular velocity as follows.

$$V_{rotor} = \omega d$$

Hence, the tip speed ratio can be expressed in terms of the angular velocity.

$$TSR = \frac{\omega d}{V_{air}}$$

The torque coefficient is defined by the following equation.

$$C_t = \frac{T_{rotor}}{T_{air}}$$

Where:

T_{air} : Torque available of the air

This torque of the air can be defined as:

$$T_{air} = F_{air}d = \dot{m}(V_1 - V_2)d$$

$$T_{air} = \frac{1}{4}\rho AdV_{air}^2$$

Hence the torque coefficient is calculated using the following equation.

$$C_t = \frac{T_{rotor}}{\frac{1}{4}\rho AdV_{air}^2}$$

Similarly, the coefficient of static torque is defined as the maximum static torque where the rotor is still at rest. This value, similar to the torque of the rotor (T_{rotor}) and the velocity of the rotor (V_{rotor}), is usually found experimentally. That is the method that was used in this design. The static torque coefficient is defined by the following equation.

$$C_{ts} = \frac{T_{static}}{\frac{1}{4}\rho AdV_{air}^2}$$

The static torque changes with the angle of attack of the wind in the rotor due to the nature of the static torque. For instance, if the turbine blade is in a position A relative to the air in which it has a smaller resistance to the air flow than in a B position then their static torque will be higher in A than in B. In other words, the air resistance is inversely proportional to the static coefficient. As a result, the static torque can be defined by the following equation.

$$T = I\alpha$$

“The moment of inertia tells us how much energy is stored in a rotating shaft or about how much energy it would take to accelerate the shaft to a particular to a particular velocity. This is called the second moment or moment of inertia and it is equal to:”

$$dI = r^2dm$$

For a Savonius turbine, the inertia of a blade can be found by:

$$I_{blade} = \int r^2 dm$$

Since the radius is relative to the angle of attack of the air in the blade:

$$r^2 = d^2 * \cos^2 \theta$$

Where:

d : Diameter of the blade (radius of the turbine)

θ : Angle of attack

While the variation of the mass can be defined as:

$$dm = \rho * h * d * t * \cos\theta * d\theta$$

Where:

h : Height of the blade (length of the turbine)

t : Thickness of the blade

Substituting the two equations in the inertia equation we have:

$$I_{blade} = \int (d^3 * \rho * h * t * \cos^3 \theta) d\theta$$

The power coefficient is defined by the equation used for Betz to determine the maximum efficiency possible. The equation is as follows:

$$C_p = \frac{P_{extracted}}{P_{available}} < 0.593$$

3.4 Boundary Layer Effect

“The boundary layer is the thin region near the surface of a body in which viscous effects are important.” (Kreith, 1999) In 1904, Ludwig Prandtl recognized that the viscous effects are

concentrated close to the surface of an object developing what is known as the boundary layer theory. The phenomenon generated is described in Figure 11. Boundary Layer growth in a flat plate, which shows how the velocity profile transforms as a result of the viscous effects. These viscous effects are the result of the friction within the fluid velocity and between the air and the flat plate.

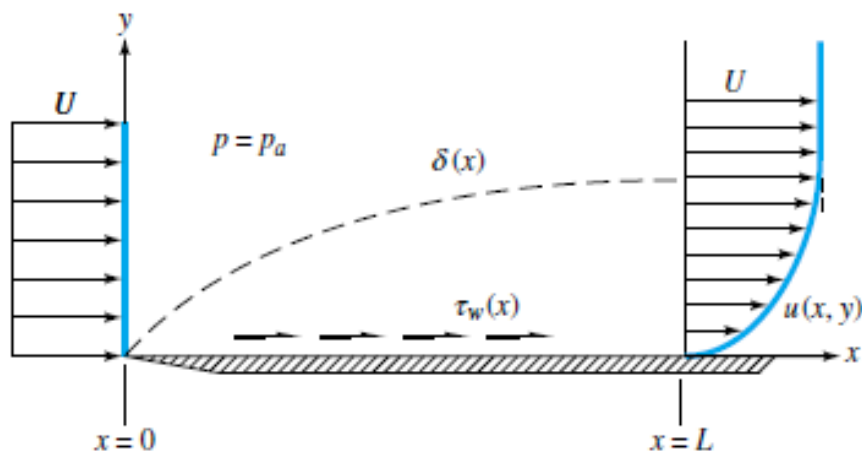


Figure 11. Boundary Layer growth in a flat plate (White, 2001)

Frank M. White shows in his book Fluid Mechanics that the momentum-integral relation for a flat-plate boundary-layer flow is defined as,

$$\tau_w = \rho U^2 \frac{d\theta}{dx}$$

Where:

ρ : Density of the fluid.

U : Velocity of the fluid.

τ_w : Shear Force.

θ : Momentum thickness.

Then by assuming that the velocity profile has an approximately parabolic shape the estimated desired thickness is,

$$\frac{\delta}{x} = \frac{5.48}{\sqrt{Re_x}}$$

Where:

δ : Laminar boundary layer thickness.

x : Position on x axis.

Re_x : Reynolds number at position x.

While the shear-stress along the plate can be calculated using the following equation:

$$c_f = \frac{\tau_w}{\frac{1}{2}\rho U^2} = \frac{0.73}{\sqrt{Re_x}}$$

Where:

c_f : Skin friction coefficient

As a result of the boundary layer, a small, but important displacement occurs in the outer streamlines. This small difference from the initial position is known as the displacement thickness of the boundary layer. The following equation defines its value.

$$\frac{\delta^*}{x} = \frac{1.83}{\sqrt{Re_x}}$$

Where:

δ^* : Displacement thickness

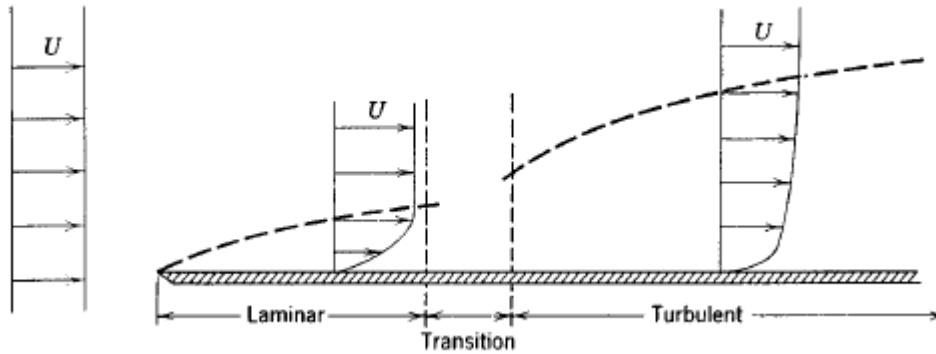


Figure 12. Boundary layer on a flat plate (vertical thickness exaggerated greatly. (Pritchard, 2011)

As shown in Figure 12. Boundary layer on a flat plate (vertical thickness exaggerated greatly., after the laminar flow, a transition section appears. In this section, the flow is neither laminar nor turbulent. The location of this section, for typical flow conditions, can be found from the following equation.

$$Re_x = \frac{\rho U x}{\mu}$$

This transition section usually can be found at $Re_x = 5000$. For instance, for a wind velocity of 30 meters per second, the section will be present at distance of $x = 0.24 \text{ m}$. (Pritchard, 2011) After this transition the fluid becomes turbulent.

“There is no exact theory for turbulent flat-plane flow, although there are many elegant computer solutions of the boundary-layer equations using various empirical models for the turbulent eddy viscosity.” (White, 2001) However, some analyses have been done that allows the calculation of approximate values for different ranges of the Reynolds number. For example, in the range of $5 * 10^5 < Re_x < 10^7$, the following equations predict the values of boundary-layer thickness and skin friction.

$$\frac{\delta}{x} = \frac{0.382}{Re_x^{1/5}}$$

$$c_f = \frac{\tau_w}{\frac{1}{2}\rho U^2} = \frac{0.0594}{Re_x^{1/5}}$$

3.5 Flow Separation

Flow separation occurs in the presence of really strong winds. In this case, the wind in contact with the plate decelerates so fast that it actually starts going in the opposite direction compared to the rest of the stream. At that point, the stream carries the wind close to the plate and a separation of fluid is generated. In other words, an empty area appears close to the plate. This flow separation obviously produces a negative pressure.

In some cases, the Kármán vortex street is generated. The Kármán vortex street is an uncommon physical phenomenon that randomly appears in nature. It consists of repetitive vortices of flow separation that can cause vibrations. At certain drag characteristics, the wake becomes unstable and begins oscillating. These oscillations or vibrations have destructive power; therefore, preventing this type of flow separation is critical.

As a result of this negative pressure, the previously discussed uplift effect appears in the roof of the houses. By redirecting and modifying the wind stream over the roof of the houses, the uplift effect can be reduced and the Kármán vortex street can be eliminated.

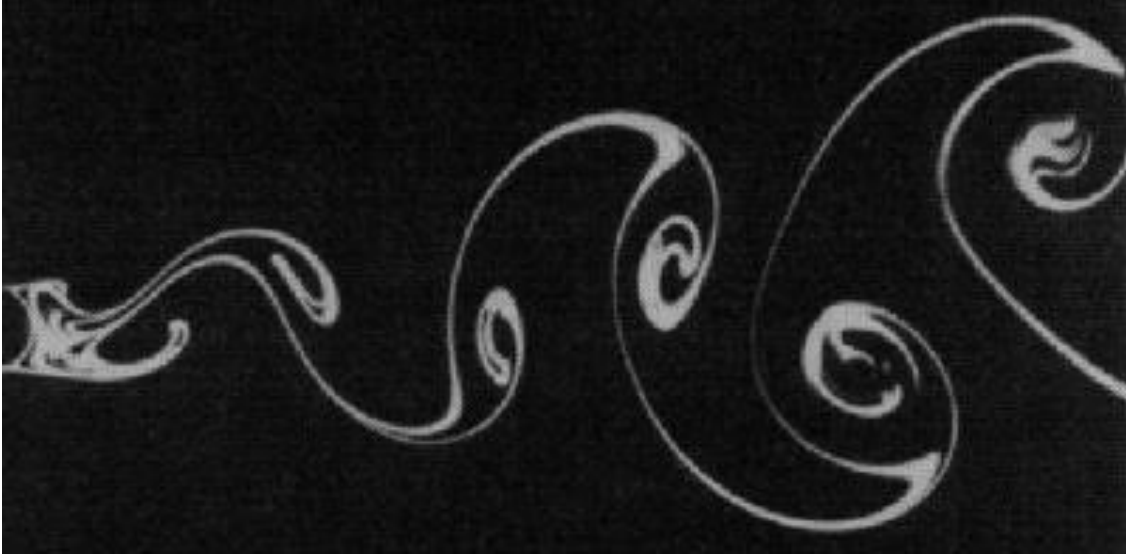


Figure 13. Kármán vortex street (ESPEYRAC & PASCAUD)

3.6 Flow pattern around a cylinder

The drag is the component of a force, parallel to the relative motion, that appears in immerse bodies. All bodies have their own drag coefficient, which varies in relation to their shape and density. The following equation defines the drag coefficient.

$$C_D \equiv \frac{F_D}{\frac{1}{2}\rho V^2 A}$$

Where:

C_D : Drag Coefficient.

F_D : Drag Force.

Given the physical characteristics of the wind turbine being designed in this Senior Design Project, it is necessary to study the flow pattern around a cylindrical object.

Contrary to what may be expected, the laminar flow usually produces faster flow separation than the turbulent flow. Although the velocities in the turbulent flow tend to be higher than in the

laminar flow, the laminar flow in a sphere generates flow separation at about 82 degrees, while the turbulent flow delays the appearance of separation to the 120 degrees (see Figure 14). This delay in the separation of the flow is the reason why the golf balls are intentionally made with indentations so that the flow around them stays turbulent and stay longer in the air.

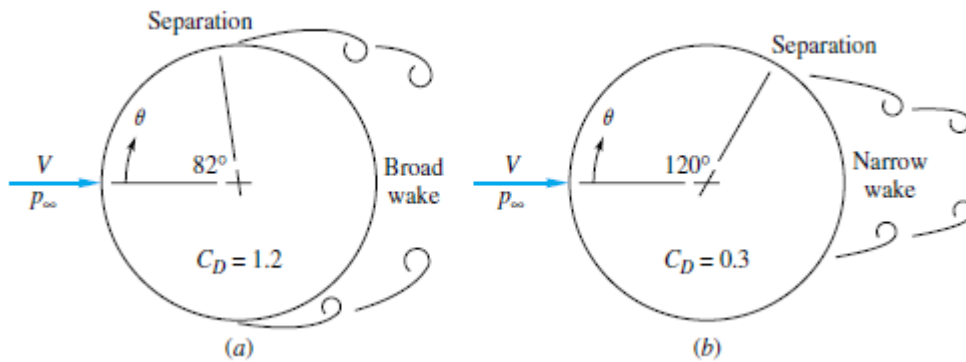


Figure 14. Separation in a sphere immersed in (a) laminar flow (b) turbulent flow (White, 2001)

Table 1. Drag coefficient data for selected objects ($Re > 10^3$) summarizes some basic shapes and their approximate drag coefficient for a Reynolds number higher or equal to 3000. This list allows the broad estimation of the value for drag that the proposed design could generate. Nonetheless, the real value should be estimated by using the previous equation.

Even though the most significant component of the force in the device is the drag, the lift also needs to be accounted for. The coefficient of lift is defined as (Pritchard, 2011):

$$C_L \equiv \frac{F_L}{\frac{1}{2} \rho V^2 A}$$

Where:

C_L : Lift coefficient

The area of a cylinder in both equations is defined as the cross-sectional area; therefore, is defined by the following equation.

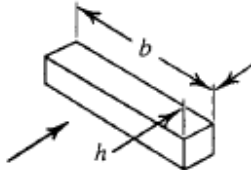
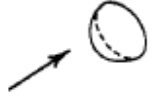
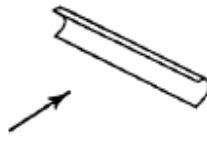
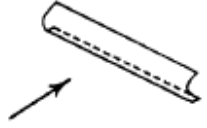
$$A = DL$$

Where:

D : Diameter of the cylinder

L : Length of the cylinder

Table 1. Drag coefficient data for selected objects ($Re > 10^3$)

Object	Diagram	$C_D(Re^{\dagger} \gtrsim 10^3)$
Square prism		$b/h = \infty$ 2.05
		$b/h = 1$ 1.05
Disk		1.17
Ring		1.20 ^b
Hemisphere (open end facing flow)		1.42
Hemisphere (open end facing downstream)		0.38
C-section (open side facing flow)		2.30
C-section (open side facing downstream)		1.20

3.7 Flow pattern around rotating cylinder

A spinning cylinder produces separation faster on its lower surface and slower on the top surface. This process generates a lift force that varies relative to the angular velocity of the cylinder. This process generates a lift force that varies relative to the angular velocity of the cylinder. For instance, for low values of spin, the lift force is actually negative; therefore, the cylinder drops faster. Alternatively, for higher angular speeds, the lift stays constant at around 0.35. This rotation does not introduce considerable changes in the drag, which remains around 0.5 to 0.6. In order to better understand the fluid mechanics of cylinders two cases are studied: in the presence of axial flow and in the presence of normal flow.

3.7.1 Rotating cylinder with axial flow

When in the presence of an axial flow through a rotating cylinder, the boundary layer is defined by its axial component and the circumferential component due to the non-slip condition at the body surface. (Childs, 2011)

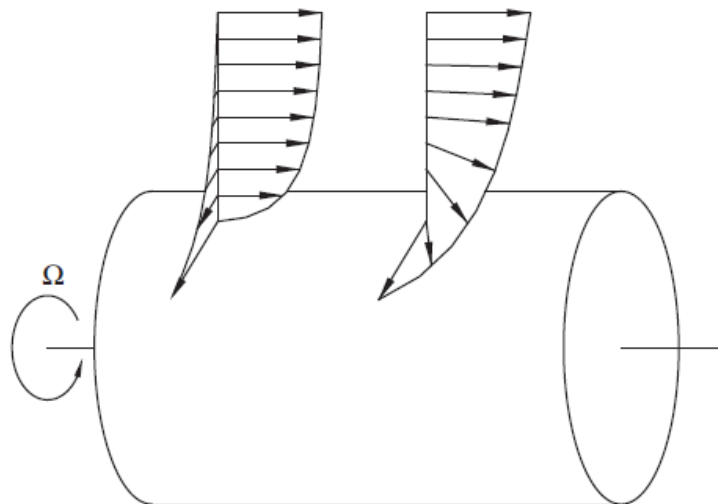


Figure 15. Boundary layer flow over a rotating cylinder with superposed axial flow. (Childs, 2011)

In this case, the thickness of the boundary layer increases as a function of the rotation parameter, which is given by the following equation:

$$\lambda_m = \frac{\Omega a}{V_{stream}}$$

Where:

λ_m : Rotation Parameter

Ω : Angular velocity of the cylinder

a : Radius of the cylinder

V_{stream} : Free stream axial velocity

An important value to be determined for the design of the device is the power required to overcome the frictional drag of the turbine when the air is flowing in a non-normal direction. This can be calculated for axial direction by using the moment coefficient for a rotating cylinder as follows:

$$C_{mc} = \frac{T}{0.5\pi\rho\Omega^2 a^4 L}$$

Where:

C_{mc} : Moment coefficient for a rotating cylinder

T : Torque required

The power is defined by the following equations.

$$P = T\Omega$$

$$P = 0.5\pi\rho\Omega^3 a^4 L C_{mc}$$

3.7.2 Rotating cylinder with normal flow

When a cylinder is rotating, and a fluid stream is acting normal to it, two reaction forces appear. One is due to the lift and other to the drag. As previously explained, the lift force is perpendicular and the drag is parallel to the flow. The flow pattern around a cylinder is described in Figure 16. Flow pattern (a) through a cylinder, (b) due to rotation, (c) combination of patterns (a). Additionally, a rotating cylinder immersed in a fluid, like air or water, generates a pattern similar to the one depicted in Figure 16. Flow pattern (a) through a cylinder, (b) due to rotation, (c) combination of patterns (b). As a result, by combining the patterns, a rotating cylinder in the presence of a moving fluid generates the pattern shown in Figure 16. Flow pattern (a) through a cylinder, (b) due to rotation, (c) combination of patterns (c).

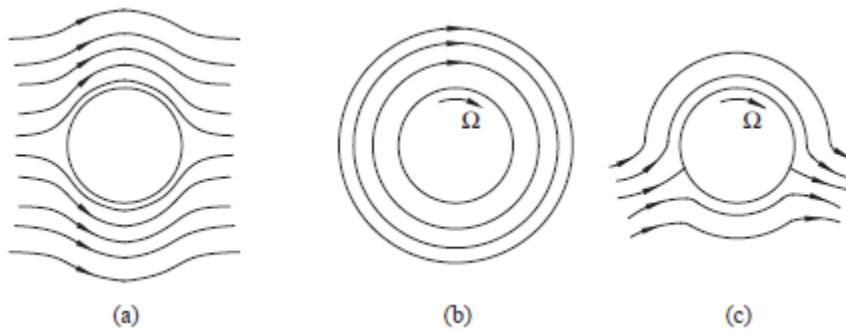


Figure 16. Flow pattern (a) through a cylinder, (b) due to rotation, (c) combination of patterns (Childs, 2011)

An important factor influencing the lift and drag coefficient, is the ratio in which the cylinder is rotating; also known as the spin factor. The spin factor is related with the drag and lift coefficient and has been deeply studied during the years. Figure 17. Lift and drag coefficients for a smooth spinning sphere in a uniform flow shows experimental results that allow the estimation of the lift and drag coefficient for a smooth cylinder. This factor is given by the following equation.

$$Spin\ Factor = \frac{\Omega r}{V_{stream}}$$

Where:

r : Radius of the cylinder

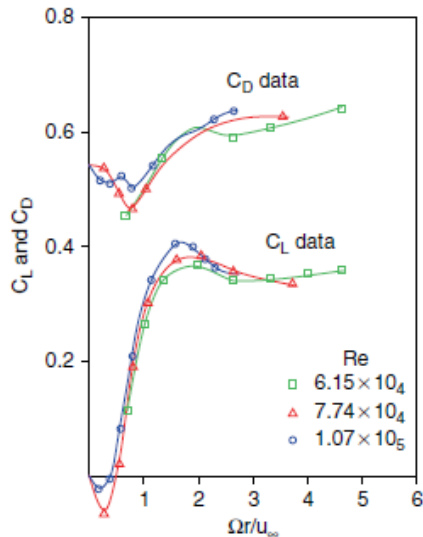


Figure 17. Lift and drag coefficients for a smooth spinning sphere in a uniform flow (Childs, 2011)

As the graph suggests, at small spin ratios the lift coefficient is small and even negative. This change in the lift and drag coefficient alters the direction and time in the air of spinning bodies. As an analogy, for this same reason, a curveball thrown with a small spin ratio might never reach the catcher. This phenomenon, in a rotating fixed cylinder, changes the direction of the fluid passing through. The flow patterns corresponding to those of the Figure 16. Flow pattern (a) through a cylinder, (b) due to rotation, (c) combination of patterns (c) are for spin ratios bigger than 2 (Childs).

As a result, a device can be designed so that when immersed in a fluid stream, it rotates and redirects the flow to compensate for the effects of separation or uplift on the roof. This device can be ideally conceived as a wind turbine with horizontal axis.

3.8 Dimensional Analysis

Most phenomena in fluid mechanics depend on geometric and flow parameters. For example, the total power available in the wind flowing through a turbine is a function of density, wind speed, and swept area. Using dimensional analysis greatly simplifies experimentation through establishing relations between these parameters without having to perform the actual experiment. To illustrate, to calculate power and torque outputs of the real size device proposed in this project, it would be necessary to build a prototype to scale. This would cost close to \$10,000, but this amount of resources is not available to the team. Nevertheless, by using dimensionless numbers, all these values can be extrapolated from those values obtained from lab experiments. Thus, by using very economical and small models at the lab, the actual values of the real turbine can be obtained.

The Buckingham-Pi Theorem is a formalized procedure for deducting the dimensionless groups appropriate for a given fluid mechanics problem. This theorem is a statement of the relation between a function expressed in terms of dimensional parameters, and a related function expressed in terms of non-dimensional parameters. In short, the Buckingham-Pi Theorem states that a relationship of n parameters of the form:

$$g(q_1, q_2, \dots, q_n) = 0$$

Can be transformed into a corresponding relationship between $n-m$ independent dimensionless Π parameters of the form:

$$G(\Pi_1, \Pi_2, \dots, \Pi_{n-m}) = 0$$

Where m is usually the minimum number of independent dimensions required to define the dimensions of all the parameters q_n ² (Pritchard, 2011).

Over the years, several important groups of dimensionless parameters have been identified. One of those parameters was explored by Osborne Reynolds in the 1880s. This parameter represents the ratio of inertial forces to viscous forces, and it was named after its initiator. In general:

$$Re = \frac{\rho V D}{\mu}$$

Reynolds discovered that this parameter is a criterion by which flow regime may be determined. Flows with large Reynolds number are generally turbulent, while low Reynolds number means more laminar flows.

Another very important number widely used nowadays is known as Mach number. This dimensionless parameter characterizes compressibility effects in a flow, and may be written as:

$$M = \frac{V}{c}$$

And can be interpreted as the ratio of inertial forces to forces due to compressibility (Pritchard, 2011).

The two dimensionless parameters mentioned above were used in this project to estimate real conditions based on results obtained from experiment. The way they were used was by setting them equal to each other for the model and the prototype. For example, the Mach number of the

² For more information about the Buckingham-Pi Theorem including how to derive the Pi groups please refer to Chapter 7 of Fluid Mechanics book by P. Pritchard.

model would be set equal to the Mach number of the prototype, and using this relationship the unknown variables on either side could be found. Section 6.1 explains this in more detail.

4. FIRST PROTOTYPE

4.1 Prototype System Description

The first prototype was built very early in the design stage for competition purposes. This prototype was presented in the RenaissanceRe Shark Tank College Competition during the 2013 FLASH Annual Conference in Orlando Florida on November 21st.

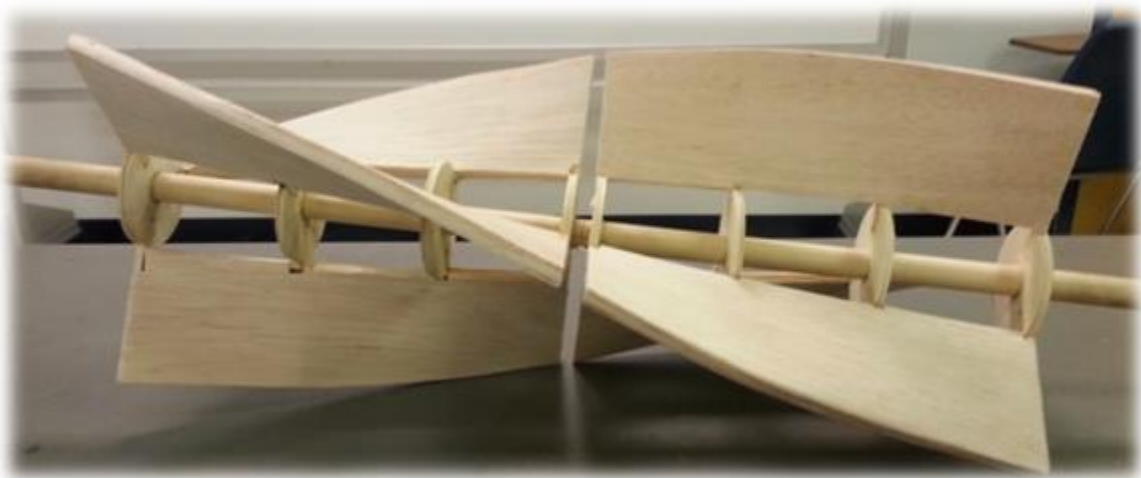


Figure 18: First built prototype

Error! Reference source not found. 18 shows an image of the first built prototype. It is a very simple model that considers the vortex characteristics of wind over roofs as explained previously.

The dimensions of this prototype are shown in Appendix A. The material chosen for construction was balsa wood. Several considerations were evaluated when choosing this material for construction. First of all, balsa wood is inexpensive, which made it an excellent candidate when compared to other materials such as harder woods, metals, or composites. Secondly, balsa wood is very soft and flexible which made the construction very simple. Finally, even though balsa is a

soft material, it provided the strength needed to fulfill the purpose of this first prototype. When all the components were attached in place, the entire turbine was strong enough to safely withstand winds of up to 20 m/s, which was the range of winds used for demonstration during the competition at the FLASH Conference.

4.2 Experimental Testing and Results

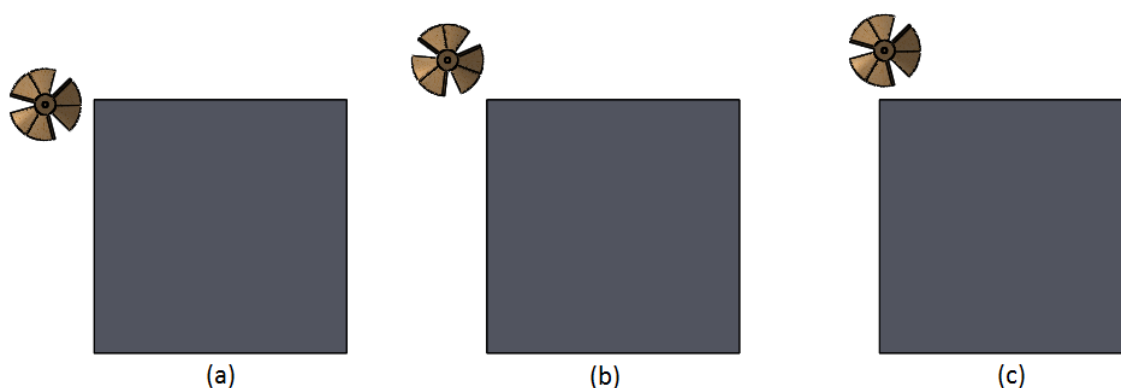


Figure 19. (a) horizontal (b) 45 degree (c) 90 degree

Several experimental tests were already performed on the prototype. For this preliminary testing stage a flat roof square house was used. One important variable considered was the position of the device relative to the roof. Three different alternatives were considered and they are shown in Figure 19. (a) horizontal (b) 45 degree (c) 90 degree. The first alternative was to place the device horizontally parallel to the edge of the roof. The second alternative was to place the device at a 45-degree angle to the edge of the roof. Finally, the last alternative studied was with the device placed at a 90-degree angle to the edge of the roof.



(a)



(b)

Figure 20. (a) experiment without device (b) experiment with device

To evaluate the efficacy of the system, the flat roof was covered with lightweight gravel, and a fan delivering winds between 5 and 10 m/s was aimed normal to the turbine and along the surface of the roof. The purpose of this experiment was to discover if this prototype was effective in reducing the pressure difference over the roof. To evaluate this, the scouring of the gravel was examined. Experiments suggested that the third alternative was the most effective in reducing the scouring of the gravel. Figure 20. (a) experiment without device (b) experiment with device20 shows the experimental results mentioned above. As the image suggest, there was a significant reduction of scouring in the gravel with the device.



Figure 21. Corner winds prototype test

Another experiment conducted using this prototype is shown in Figure 21. Corner winds prototype test21. For this experiment, the fan (shown in blue in the picture) was placed at a 45-degree angle with the roof. The purpose of this experiment was to be able to observe the difference of the scouring with and without the device in one single experiment. As the picture suggests, the gravel on the side of the roof

without the device was almost whipped out completely, while the edge of the roof with the turbine was almost intact. These results demonstrate that the system works, which was the main purpose of all experimentation up to this point.

5. DESIGN STUDY

In order to arrive to the best possible alternative for the design, a series of steps were performed. To analyze the validity of the idea, the progression of the results were shown through the improvement and fulfillment of the objectives of this report. In other words, these series of steps show how the wind uplift effect and the flow separation are improved as the geometry of the design changes. Furthermore, power generation is either increased or maintained similar as the design is improved.

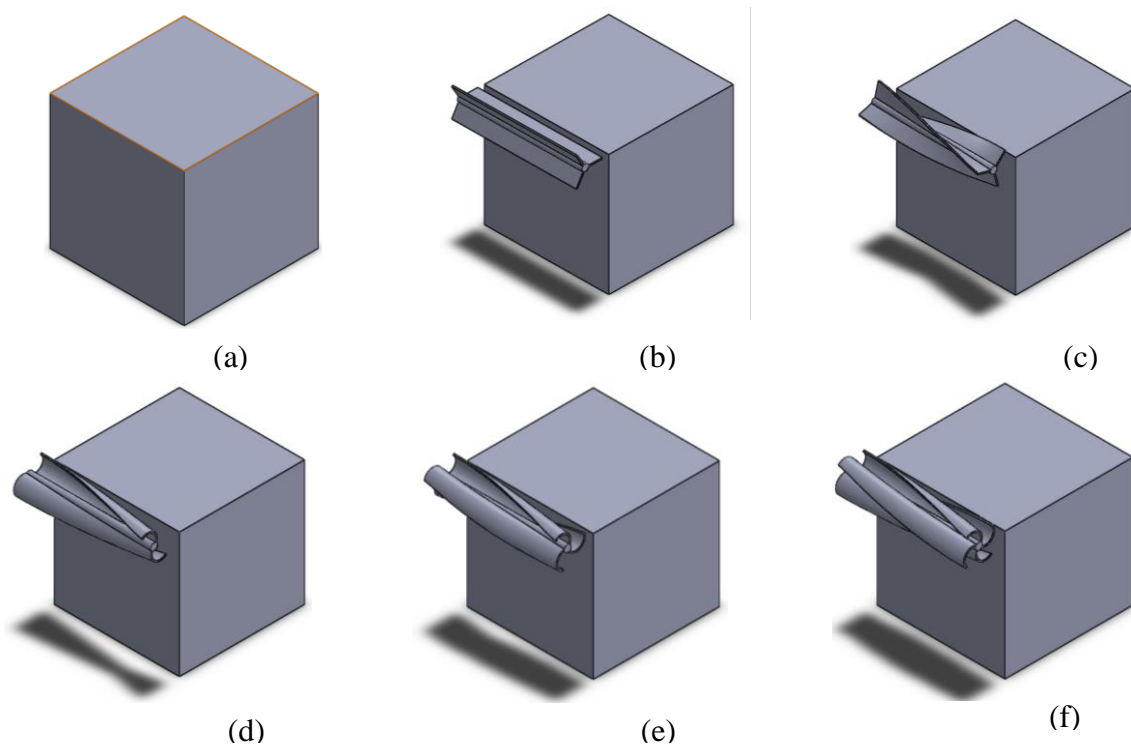


Figure 22: Analysis progression. (a) House alone. (b) House with straight blade turbine. (c) House with twisted straight blade turbine. (d) House with twisted 2-blade Savonius turbine. (e) House with twisted 3-blade Savonius turbine. (f) House with twisted 4-blade Savonius turbine

The first step considered from the design point of view was to place the house alone in the study area. The second step was to utilize a straight blade turbine as shown in Figure 22b. This was the first type of turbine studied because it is the simplest one. Straight blade turbines are the simplest in terms of design as well as ease of manufacturability. After this second step was performed, it was compared to the previous result. The next step was to give a twist to this straight blade turbine and observe the improvement. The final step was to utilize three different types of Savonius turbines and observe the differences between them, and the other two types. These steps follow a logical path that started with the simplest possible shape, and evolved into more advanced shapes such as Savonius. The latter has been proven to yield very high efficiencies for power generation, which was also an objective of this project.

To assess the validity of the results, two experiments were performed. First of all, a CFD analysis using ANSYS was performed to validate the results numerically. ANSYS is a software widely used for computational fluid dynamics (CFD) analysis; and it is one of the most effective and accurate programs to simulate fluid flows. Additionally, ANSYS can be used for other applications as well. In this case, ANSYS Fluent is very useful due to its extended capabilities, which can model adjustable meshes and allows the analysis of the results by modifying the settings without causing further delays. Secondly, actual experiments were performed at the Transport Phenomena Laboratory at Florida International University. This laboratory has a wind tunnel that is capable of achieving velocities of up to 60 km/h, which was very useful for the purpose of this project.

Nevertheless, before any of the above mentioned steps were taken, a series of preliminary experiments were performed.

5.1 Initial Analysis: Using Straight Blade Turbine

Although the analysis with the cylinder was intended to be the initial step, the first analysis performed towards progression study was to determine the best possible number of blades of a straight blade turbine; as well as the best possible diameter to length ratio of it. It is important to note that the length was not a parameter considered for the study, but instead was used to determine the aforementioned ratios. The analysis was performed using two methods: experimental and computational.

Based on the wind turbine geometry analysis, the relationship between turbine diameter and length was obtained by setting the following relation:

$$b = k * D$$

Where,

b: Interior Length

k: Ratio between interior length & tip-to-tip distance

D: Tip-to-tip distance

The relationship length & tip-to-tip distance is defined by the following equation:

$$0.12 = b * D$$

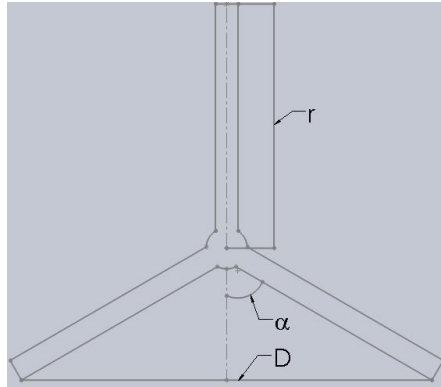


Figure 23: 2D wind turbine front view

Figure 23 represents a two dimensional cross section of a three-dimensional flat blade wind turbine. The angle (α) was defined between the wind turbine blade and the “Y” axis. Furthermore, a value for the interior length (b), tip-to-tip distance (D) and radius (r) was calculated for different values of $k = 1, 2, 3$; as well as number of blades 3, 5, 7. The results of these calculations are shown in the table below.

Table 2. Design parameters for prototype calculations

K	D [m]	b [m]	No. of Blades		
			3	5	7
1	0.105586	0.1056	r [m]	r [m]	r [m]
2	0.07466	0.1493	0.06096	0.05551	0.05415
3	0.06096	0.1829	0.04311	0.03925	0.03829
			0.03520	0.03205	0.03126

5.1.1 Initial Mesh Study

The purpose of this initial study was to determine the best possible mesh for the simulations. The following procedure is a detailed step-by-step method for performing these analyses using ANSYS Fluent.

- 1) Open ANSYS Workbench

- 2) Double Click on Fluid Flow (Fluent)
- 3) Right Click on “Fluid Flow (Fluent)”, and Click on Properties
- 4) Click on Geometry
- 5) On the panel to the Right, select 2D

GEOMETRY

- 6) Double Click on Geometry, the Design Modeler will open. This modeler allows the user to draw a sketch from scratch, but it also allows the user to import a solid from SolidWorks, which is more user-friendly for drawing.
- 7) Go to the menu, click on File/Import External Geometry File
- 8) Select the Geometry file previously drawn in SolidWorks (to avoid errors and simplify the import, save the SolidWorks model as a .STEP file)
- 9) Click Generate (This operation needs to be repeated after every change)
- 10) Click on Concept/Surface from Faces
- 11) Select the Face that needs to be studied on 2D. (Make sure that the Operation stays as Add Frozen)
- 12) Click on Apply, and then click on Generate. Two parts and two bodies will appear, keep the face, and suppress the model.
- 13) Right Click on the part that contains the model and suppress; and then on the Modeling menu click on the plane that contains the newly created surface.
- 14) Click on New Sketch
- 15) Click on the Sketching Tab, Select a Circle and draw a circle that reaches until the outside the turbine profile. This sketch needs to be bigger than the profile and it is required only

for moving frames or moving mesh. In other words, if the intention is to create a simulation with the object moving, this has to be done.

- 16) Click on Dimensions/Diameter, and then click on the circle and then anywhere on the drawing screen.
- 17) Change the Diameter value on the Details View menu. If needed, select any of the zoom buttons.
- 18) Click Generate, and then Concept/Surface from Sketches
- 19) Click on the Sketch, then Apply, and then Generate. (Change Add Material to Add Frozen)
- 20) Click on New Sketch (now repeat the same procedure to create a new sketch)
- 21) Create a Rectangle. (The dimensions of this rectangle need to have the same dimensions of the real life situation that is being simulated. In this case it has the same dimensions of the Wind Tunnel that was used to test the prototypes.)
- 22) Define the Dimensions, Click generate.
- 23) Click on Concept/Surface from Sketch
- 24) Click on Create/Boolean
- 25) Change the Operation to “Subtract”.
- 26) Set the rectangle as the target body, and the circle as tool body. Click on the Target Body and then the Rectangle, click Apply. Then click on Tool Bodies and then the Circle, Apply. Change the Preserve Tool Bodies to Yes. Click Generate.
- 27) Repeat the operation, and this time select the circle as the Target Body, and the turbine surface (previously created from the turbine surface) as the Tool Body. Leave the Preserve Tool Bodies with No. Click Generate.

In ANSYS FLUENT, the solid behaves like an empty space. Since the analysis is done on the fluid (air, water, etc.), what happens inside the wall is not important. By leaving the solid as an empty space its perimeter can be declared as a wall.

- 28) Click on the rectangle and in the Details View, change the Solid to Fluid. Repeat this operation for the Circle.
- 29) Go to the selection tools and Click on the Select Edge button.
- 30) Left Click on the left edge of the Rectangle to select that edge. Right click on it, and select Named Selection Option.
- 31) Change the name to velocity_inlet and click Generate.
- 32) Repeat this operation for the following edges and planes using the following names. (To select more than one edge at the time, press and hold the Control Button)
 - a. Right Edge of the rectangle pressure_outlet
 - b. Top and Bottom Edges of the Rectangle wall
 - c. The Circle edge (only the circle) circle_interface
 - d. All the edges of the Profile turbine
 - e. Rectangular Area air_windtunnel
 - f. Circular Area air_turbine

If the experimental conditions do not match with the closed section of this wind tunnel, use the term Symmetry. These names may seem random, but words like inlet, outlet, wall, and symmetry are recognized by ANSYS as commands and will facilitate the setup and simulation steps.

- 33) Click on File/Save Project
- 34) Select the location of the Project and Save

MESH

- 35) Double Click on Mesh
- 36) Click on Generate Mesh

Some of the following steps can be modified in order to complete a Convergence Study for the simulation. Nonetheless, the initial mesh is always too coarse to get a good result, so the following steps are recommended.

- 37) Right Click over Mesh. Click on Insert. Click on Method.
- 38) Click over the Rectangle and the Circle. Click on Apply.
- 39) Change the Method to Triangles.
- 40) Click on Generate Mesh.

For Air flow, it is recommended the triangular mesh because it adjusts better to figures like circles and airfoils.

- 41) Left Click on Mesh, click over the plus button on Sizing. Here two things can be modified. First, the Relevance Center, which is in Coarse, can be modified to Medium or Fine. Second, the Smoothing can be modified from Medium to High
- 42) Right Click on Mesh. Click on Refinement. Click on Select Edges. Press and hold Control and select all the edges of the turbine by left clicking over them. Click Apply.
- 43) Change Refinement to 3. Click on Generate Mesh
- 44) Repeat the Refinement Operation, but this time click on select faces and select the Circle and the rectangle. Now the mesh around the turbine is really fine, but the circle_interface is too different.

- 45) Right Click on Mesh. Click on Sizing. Click on Select Edge. Click on the edge of the Circle. When this edge is selected the program shows a double layer icon in the modeling area. Press and hold control and click on the second rectangle.
- 46) Click Apply. Change the Type to Number of Divisions and set it to 100.
- 47) Save the Project and close the Meshing Console.

SETUP FOR STEADY STATE STUDY

- 48) Double Click on Setup.
- 49) Click on Double Precision. Click Ok.
- 50) Click on the Check Button to Check the Mesh.
- 51) Select Type as Pressure-Based, Velocity Formulation as Absolute, Time as Steady, and 2D Space as Planar.
- 52) Click on Models
- 53) Double Click on Viscous-Laminar.
- 54) Select the K-Epsilon unless a more specific solution is required. Click on Realizable. Click on Non-equilibrium wall functions. Click Ok.
- 55) Click on Materials. In this step it is necessary to define the materials. ANSYS has some materials in the program database, but if it does not have the one you need you can follow this procedure.
- 56) Click the material you want to replace. Click the Create/Edit Button.
- 57) Click on User-Defined Database

- 58) Enter any name for your database and Click Ok. When ANSYS asks if you want to create a database click Ok.
- 59) Click on New. Enter the name, Formula, Type, and any other material property that is available.
- 60) Click on each material property, and then click on edit. Edit the value of each property. Once the material is added it will appear in the list.
- 61) Click on Cell Zone Conditions
- 62) Click on Frame Motion. Leave X(m) and Y(m) as zero. Change the rotational velocity to the value required.
- 63) Click on Boundary Conditions
- 64) Click on pressure-outlet, and then click edit. Notice that the gauge pressure is zero. This value only means that the pressure at that point is equal to one atmosphere.
- 65) Click on turbine, and then click edit. Click on Specified Shear. Unless the shear stress is known, leave it at zero. This operation is repeated to all walls in the setup.
- 66) Click on velocity_inlet, and then click edit. Set the velocity magnitude with the desired velocity. Notice that the direction of the flow can also be changed by changing the velocity specification method.
- 67) Click on Mesh Interfaces. In this window the user should check the interface between the two regions of mesh that were created.
- 68) Click on Reference Values and choose to compute from velocity_inlet.

SOLUTION

- 69) Click on solution method.
- 70) Changer the Turbulent Kinetic Energy and the Turbulent Dissipation Rate to Second Order Equations.
- 71) Click on Solution Initialization.
- 72) Click on Standard Initialization. Change to Compute from velocity_inlet. Click on reference frame absolute. Click on Initialize.
- 73) Click on Run Calculation
- 74) Set the number of iterations.
- 75) Click Calculate.

RESULTS

- 76) Click on Graphics and Animations
- 77) Click on Contours. Click on Set Up.
- 78) Click on Filled. Change to Velocity. Click on Display.

In this last window many different results can be set from path lines to contours and from pressure to velocity.

FOR TRANSIENT STUDY

Follow the prior procedure up to step 52.

52. Select Type as Pressure-Based, Velocity Formulation as Absolute, Time as Transient, and 2D Space as Planar.

Continue with Step 53 of the prior procedure until Step 63

63. Click on Mesh Motion. Leave X(m) and Y(m) as zero. Change the rotational velocity to the value required.

Continue with Step 64 of the prior procedure until Step 68

68. Click on Mesh Interfaces. Click on Preview Mesh Motion. (Verify that your mesh/turbine is rotating the right way)

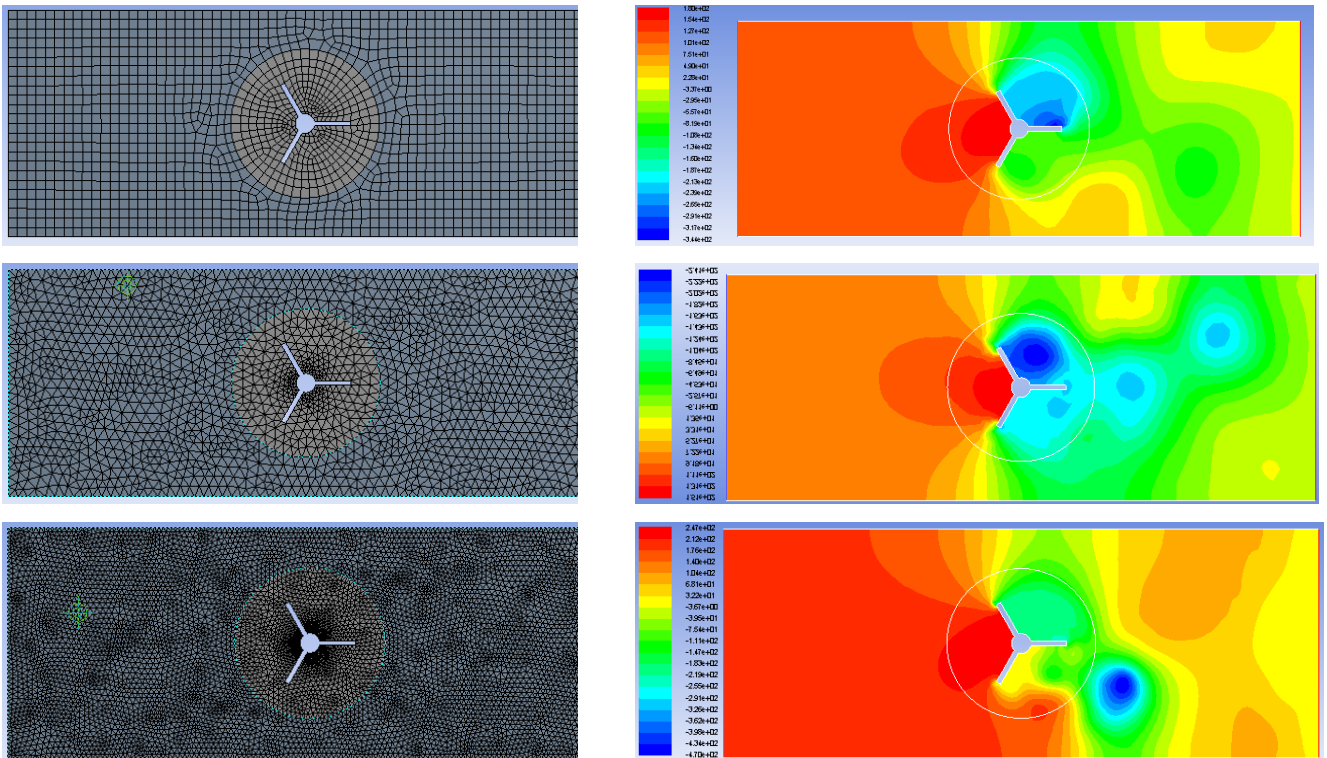
Continue with Step 69 of the prior procedure until Step 74

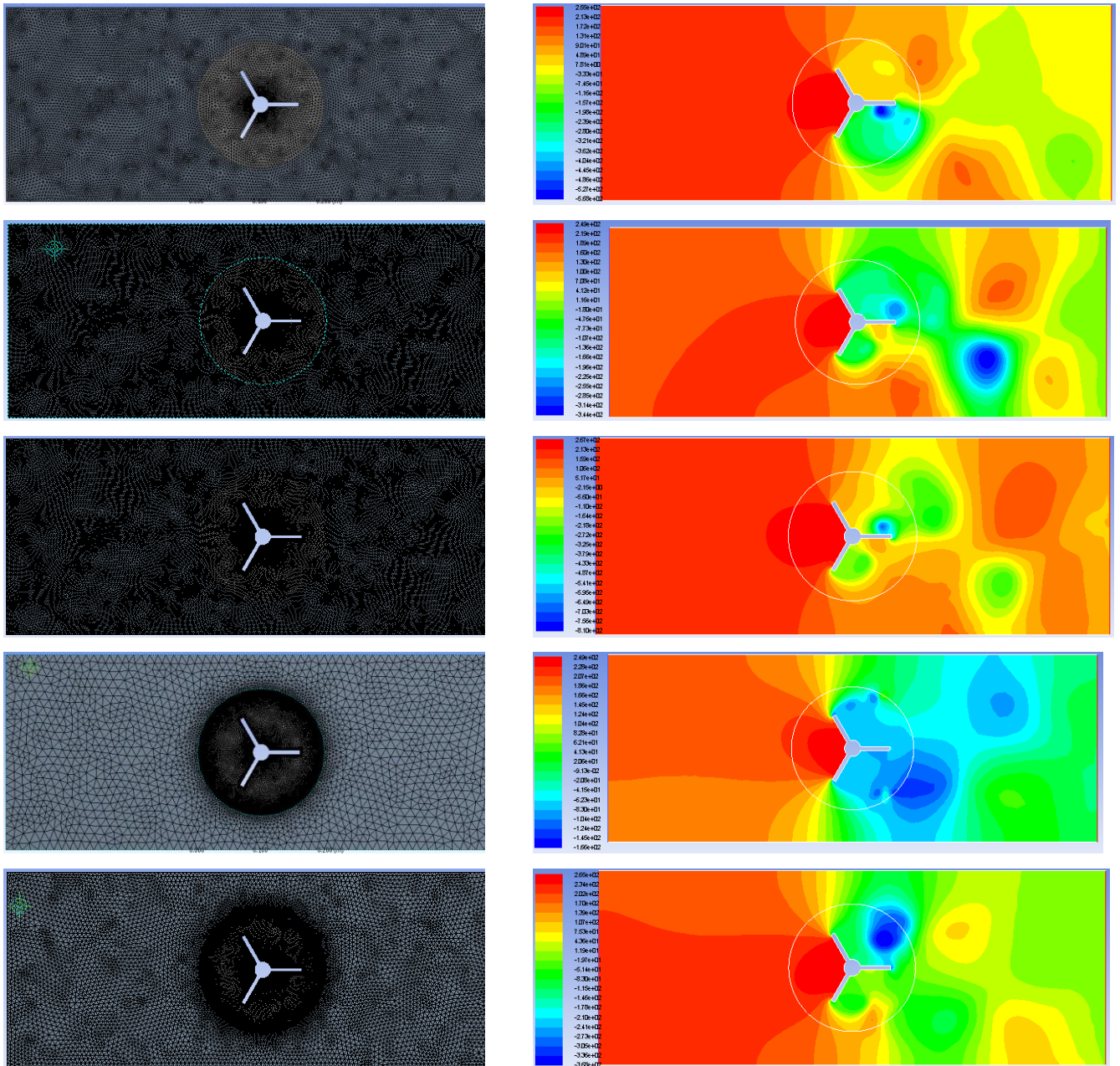
74. Click on Calculation Activities. Go to Solution Animations, click on Create/Edit
75. Change Animation Sequences to 1 or more. Each individual sequence needs to be defined.
76. Change from Iteration to Time Step.
77. Click Define
78. Click on Contours
79. Change from Pressure to Velocity or other desired plot.
80. On options, activate Filled and Node Values; unselect the other options.
81. Set the range of the velocity for the plot. Take into account that if your range is too big or too small the results will not be appreciable.
82. Click on Display. Click on Close. Click Ok.
83. Click Ok.
84. Click on Run Calculation.
85. Set the time step, the number of steps, and the max iterations/time step.
86. Click on Calculate.
87. Click on Graphics and Animations

88. Go to Animations. Click on Solution Animation Playback. Click on Set Up.
89. Click on Play. At this point the simulations should provide a transient animation, which the user can convert into a video by changing the Write/Record Format Option of this window. The validity of these results depends on the Analysis constraints, and the Physical Characteristics of the Experimental Analysis.

This concludes the Analysis.

The following series of images represents the mesh studies performed to determine which of the mesh used yielded the most accurate results. For each pair, the picture on the left is the mesh used, and the picture on the right is its corresponding pressure profile after simulation.





Analysis of the results showed that the last mesh was the best configuration. Thus, using the selected mesh, a deeper study was performed in which the cases shown in Table 2 were evaluated. Following the study, the results suggested that the turbine with three blades when $k = 1$ was the best one among all. The reason was that it offered the best pressure

distribution after the turbine. However, this study was still a little far from the designed lab experiment, thus a new study was performed.

5.1.2 Finding Best Number of Blades, Using Improved Geometry and Mesh

In this new study a block was added behind the turbine to simulate the house, and the configuration of the geometry was also changed to accommodate this “house.”

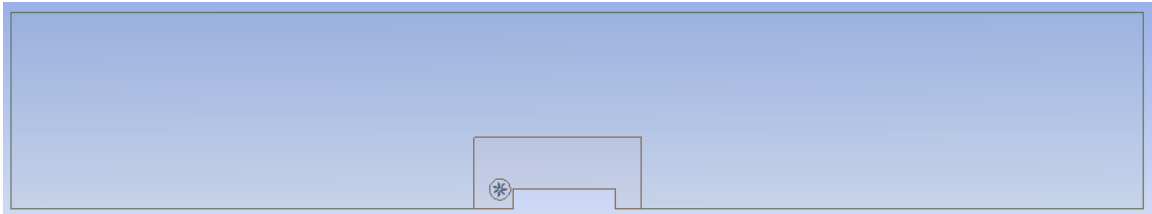


Figure 24: Study geometry with house

As Figure 24: Study geometry with house4 shows, the outermost rectangle represents the wind tunnel, and the innermost rectangle represents the house behind the turbine. The other rectangle enclosing the house as well as the circle enclosing the turbine was added for meshing purposes. For this particular study, the dimensions used were not exactly similar to those of the actual experiment. The length of the wind tunnel, as well as the length of the house used was longer than the length used for the experiment. The reason this study was performed, using different dimensions, was to try to improve the results provided by ANSYS. However, it is important to note that this particular procedure was done only to determine the best possible number of blades of the turbine. This best number of blades was chosen from the 9 cases studied, and the difference in length does not affect this decision.

The first most important step to complete this study was to select the best possible mesh based on previous experience. The following figure shows the final mesh using the geometry shown in Figure 25: Improved geometry and mesh for initial study4.

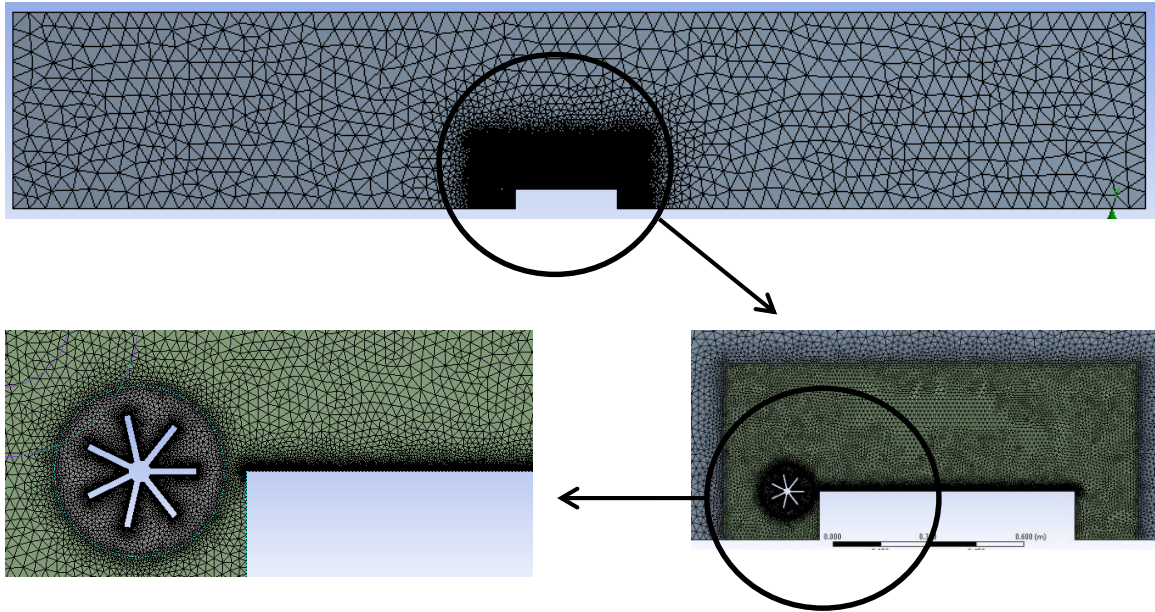


Figure 25: Improved geometry and mesh for initial study

The following bullets describe some of the most important characteristics of the mesh shown in Figure 25:

- The field before and behind the house uses a larger element size. This was left like that to save computing time. Nevertheless, since there was not much change in this field, the element size used was good enough to yield accurate results.
- The “house” and the turbine were enclosed in a square that has a much smaller element size. This was done to account for any sort of turbulence and changing behavior of the fluid after going through the turbine. Also, this was the area of interest of this project, thus it was important to have the best possible results here.

- A very small mesh was used around the blades of the turbine. The reason for this was because the turbine was spinning at a very high rate of 31.4159 rad/s; thus it was important to have a mesh that would guarantee accurate results.
- Finally, a very small mesh was used at the roof of the house. This was the most important part of this study because the pressure distribution along the roof of the house determined whether or not this new concept was effective. The element size used at the roof of the house was of 0.0001 m.

It is important to mention how the element size on the roof was selected. The analysis behind choosing this element size lies in the concept of the boundary layer. The element size on the roof was chosen to be at least as small as the boundary layer at 1 mm from the edge of the roof; and at least 1/5 of the boundary layer at 1 cm from the edge of the roof. As explained in section 3.4, the boundary layer has a laminar portion, followed by a transition portion, and by a turbulent portion. The interest of this project is to observe what happens in the laminar and transition portions of it. Thus, the maximum x-coordinate was chosen as the one corresponding to $Re_x = 4 \times 10^5$, which is the limiting value between transition and turbulent boundary layer. The boundary layer was calculated using the following equation:

$$\frac{\delta}{x} = \frac{5.48}{\sqrt{Re_x}}$$

As the equation shows, the boundary layer thickness is a function of the position from the edge of the roof, x, as well as the Reynolds on x. The following table was constructed using these equations:

Table 3: Boundary layer thickness calculations

x [m]	Re _x	δ [m]
0.001	6.18E+02	0.0002
0.005	3.09E+03	0.0005
0.01	6.18E+03	0.0007
0.02	1.24E+04	0.0010
0.03	1.85E+04	0.0012
0.04	2.47E+04	0.0014
0.05	3.09E+04	0.0016
0.06	3.71E+04	0.0017
0.07	4.32E+04	0.0018
0.08	4.94E+04	0.0020
0.09	5.56E+04	0.0021
0.1	6.18E+04	0.0022
0.2	1.24E+05	0.0031
0.3	1.85E+05	0.0038
0.4	2.47E+05	0.0044
0.45	2.78E+05	0.0047
0.485	3.00E+05	0.0049

Once the mesh was selected, the next step was to evaluate all 9 cases shown in Table 3: Boundary layer thickness calculations². The following graph shows the results obtained from this study.

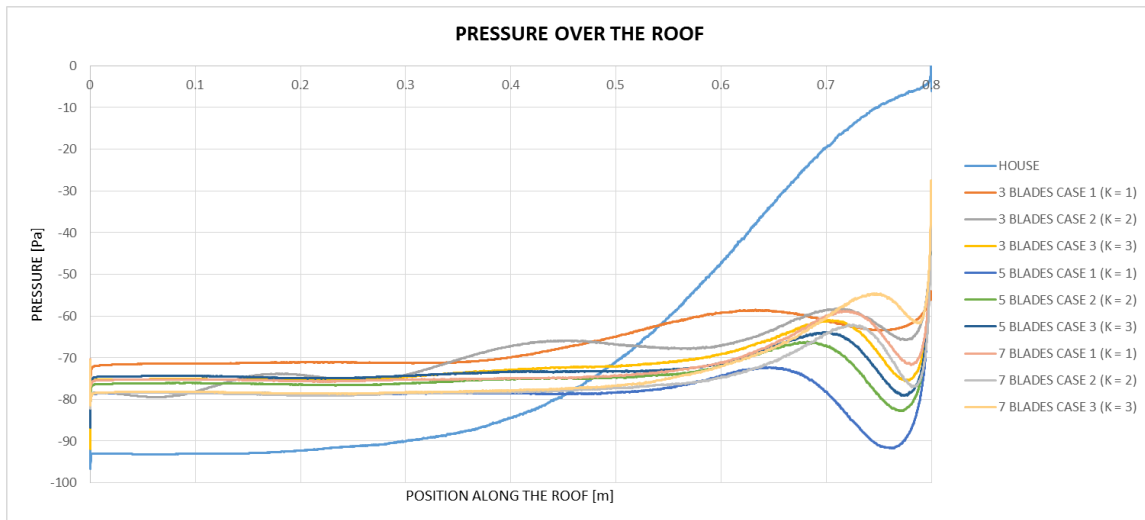


Figure 26: Pressure over the roof of the house for improved geometry and mesh study

The graph above shows the pressure values along the roof for all the cases including one line for the roof alone. As the graph suggests, there was an improvement in the pressure when any of the devices were attached to the house. This improvement can be seen by the higher pressure achieved, and also by the much more stable pressure distribution. However, the purpose of this study was to select the best possible number of blades to move on to the next step of the project. Thus, by analyzing the data provided by this graph, it was seen that the turbine with three blades yielded the best results. Thus, for the remaining of the project and subsequent analyses, that was the only case considered for a straight blade turbine.

5.1.3 Finding X and Y Position of the Turbine in Relation to the Roof of the House

Having defined the number of blades for the straight blade turbine as 3, the position of the turbine was also studied through ANSYS. To complete this analysis all the parameters of the experiment were maintained with the exception of the X and Y center position of the turbine with respect to the house. Table 4. X and Y offset positions contains

all the positions in X and Y used to find a precise location in which the improvement on the pressure profile along the roof was notable. The method of selection of a suitable position in X and Y for the center of the turbine was by comparison of the pressure profiles along the roof. The comparison showed the smaller pressure difference, and that position was then used for the rest of the analysis.

Table 4. X and Y offset positions

X	Y
0.005	0.06096
0.01	0.04572
0.015	0.03048
0.02	0.01524
0.025	0
0.03	-0.01524
0.035	-0.03048
0.04	-0.04572
0.045	-0.06096
0.05	

The results of the simulations with the different X values are shown in the figure below. From that image it can be appreciated that the turbine improved the pressure profile on the roof, when the position was changed from 0.005 to 0.025 meters. Nevertheless, the position with the best profile was for an X value of 0.015 meters.

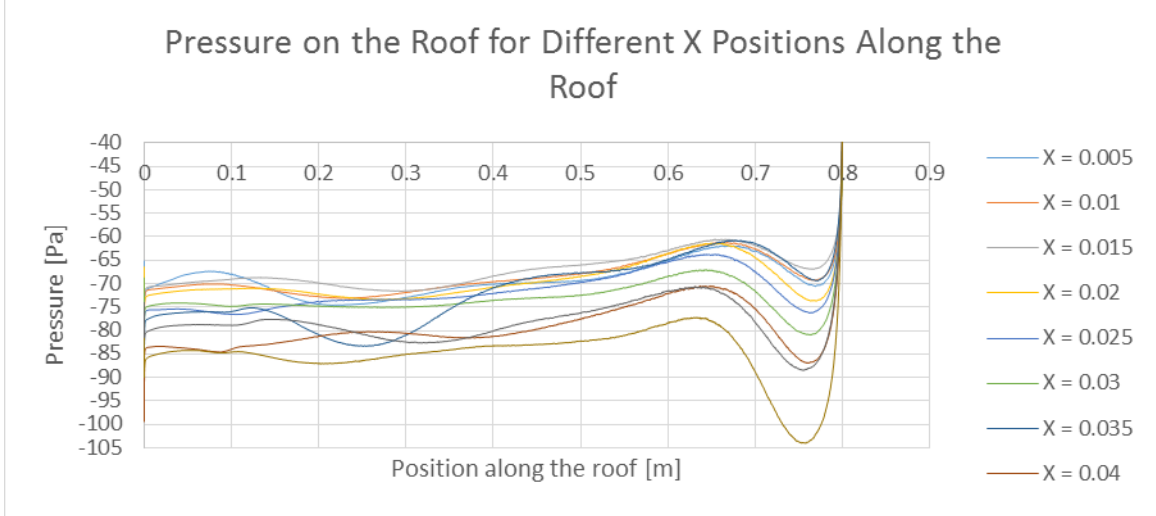


Figure 27. Pressure profiles for different X positions

Figure 28. Pressure profiles for different Y positions shows the results for the simulations with different Y center positions for an X value of 0.015 meters. From the comparison it was derived that the axis of the turbine can never be below the roof. If this happens, it introduces vibrations in the roof, and the pressure on the roof could be aggravated instead of mitigated. On the other hand, there are a range of acceptable values between the 0 m position, or roof aligned, and the 0.03048 m which is half of the radius of the turbine. However, to avoid complications during the experiment the Y position of the shaft of the center of the turbine was maintained at the 0 value.

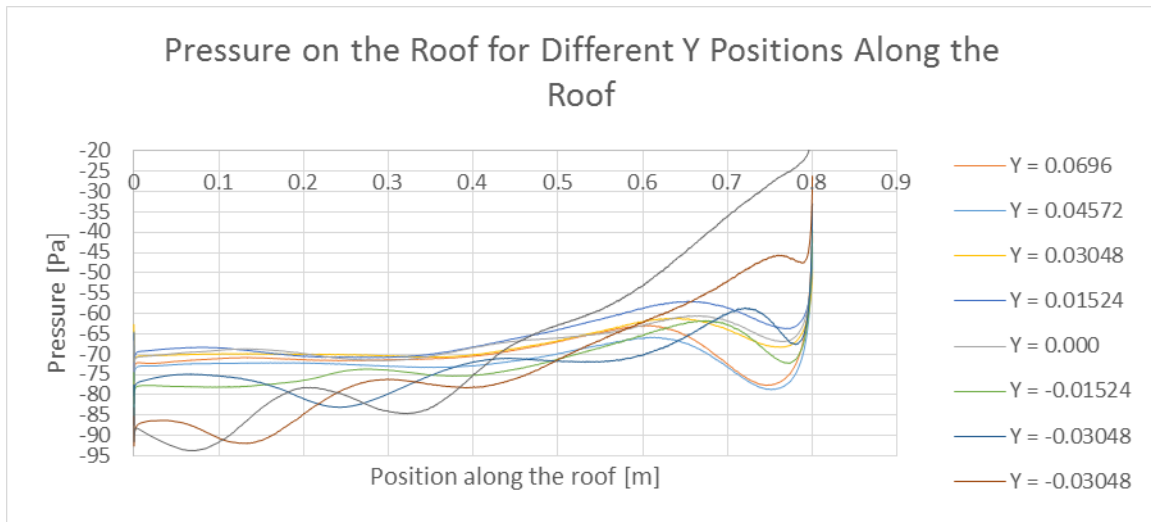


Figure 28. Pressure profiles for different Y positions

5.2 Computational VS Experimental Results: Progression Study

This section of the present senior design thesis report shows the results obtained from experiments as well as from simulations using CFD.

Once the best possible number of blades and the position of the turbine with respect to the house were decided upon, the next step was to perform a progression study. This progression study is shown in Figure 22. There were six different studies performed, and they are individually presented next. There is one subsection entirely devoted to each of these studies, where the results obtained were analyzed and compared.

5.2.1 Initial Experimental Setup

This is an introductory section that explains in more detail the setup for all experiments.

The experiments were performed using the Subsonic Wind Tunnel Instrumentation System in the Transport Phenomena Laboratory at FIU Engineering Center. This wind

tunnel has a working range of wind velocity from 0 to 11 m/s. The same was calibrated to manufacturer specifications prior to the experiment.

In order to perform an experiment that could be further validated and compared using CFD, the velocity profiles of the working area were studied as an initial step. These profiles were determined in order to choose a portion of the area providing constant velocity. The following graph contains the velocity profiles showing that more than the 50 percent of the wind tunnel width provides similar velocities. The curves were plotted in a graph showing Velocity VS frequency of rotation of the fan.

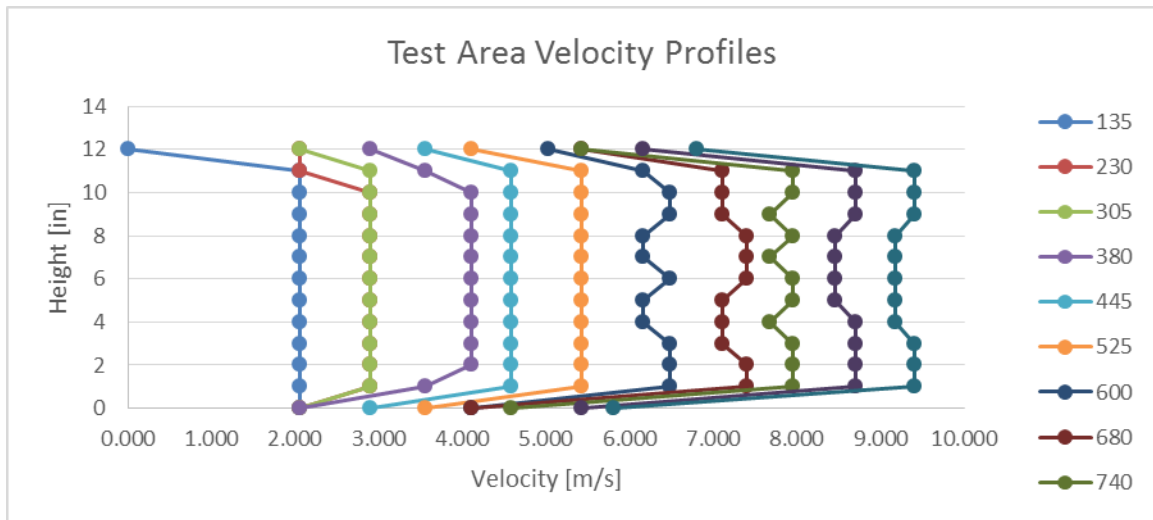
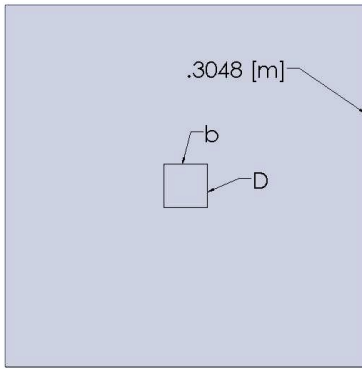


Figure 29. Velocity profiles in the wind tunnel

One of the main restrictions when using the wind tunnel was the available (total) cross-sectional area, with a value of 0.9290 m^2 . In order to avoid the boundary layer effects on the velocity profile inside the wind tunnel, only a certain percentage of the total area was used for the experiments. For this particular project, a safe value of 12% of the cross-

Figure 30: 2D cross-sectional area of the wind tunnel



sectional area was used for the analysis. Using such a small portion of the total cross-sectional area means that the velocity profile remains almost constant in this range. This is shown in Figure 30, where the small square in the center represents the area used for the experiment (not drawn to scale.)

Additionally, the velocity in the wind tunnel was studied using two different methods. First of all, the dynamic pressure was measured with a pitot-tube, and the pressure then calculated using an Extech 45160 airflow meter. Then, the same velocities were directly measured using a tachometer. The values of the velocities were calculated and compared in the graph below.

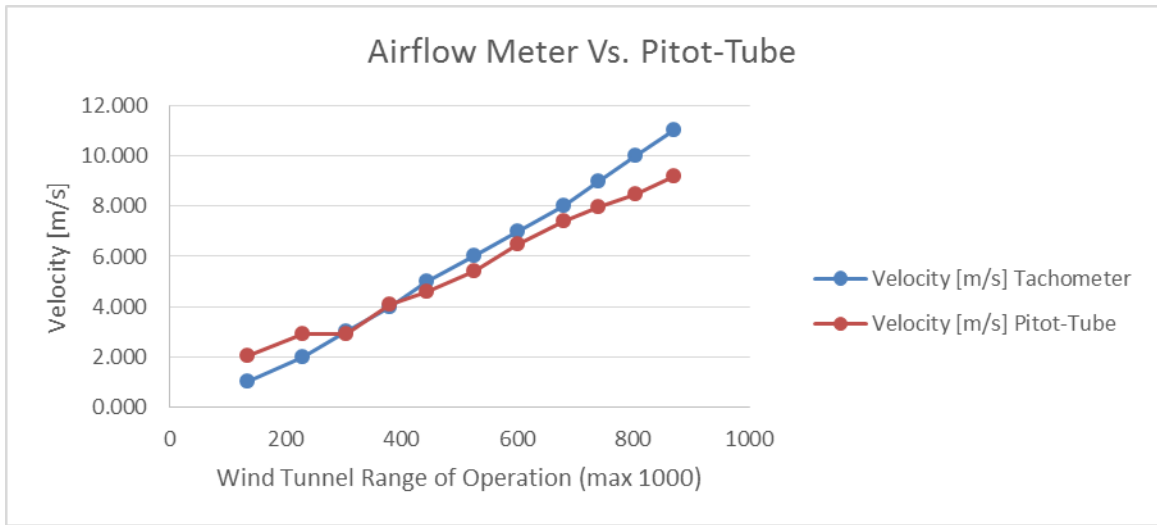


Figure 31. Velocity airflow-meter vs. Pitot-tube

As the graph suggests, both curves are very close to each other, with a very small difference between them. For that reason, these values were assumed to be good enough for the purpose of the preceding experiments.

The different mini-turbines used for experimentation were modeled using Solidworks and then 3D-printed using a Makerbot Replicator 2. This printer has the following specifications (Makerbot Website Faq, 2014).

- 100-micron layer resolution.
- Very large build volume: 410 in³ (11.2 L x 6.0 W x 6.1 H in) / 6691.0 cm³ (28.4 x 15.5 x 15.2 cm).
- MakerBot PLA Filament, a bioplastic derived from corn.
- Professionally engineered and expertly built for speed.
- Pop-out build platform for convenient print retrieval.
- New MakerBot MakerWare software that speeds the 3D printing process.

The study area of the wind tunnel has a small orifice in the back acrylic wall that allows for an airfoil or other body to be fixed in place by using some sort of shaft, and inserting this shaft into the orifice. As a result, and to avoid unnecessary friction during the experiment, miniature steel shaft and bearings were used. The steel shaft was selected based on the diameter of the orifice, while the bearings were selected based on the shaft diameter and the maximum number of RPM expected. These parts were bought from McMaster.com. Their description and part number appear below.

- Mini High-Precision Stainless Steel Ball Bearing - ABEC-5, Standard Open, 3/16" ID, 5/16" OD, .109" Width (57155K352)
- Miniature 12L14 Drive Steel Shaft, 3/16" OD, 18" Length (1327K54)

The setup could not be completed without adding a square house with flat roof to simulate a real life condition. The house was designed with half the section of the wind

tunnel to coincide with the X and Y positions previously determined through ANSYS simulations. The house had two main functions: first to reproduce the air flow pattern around the turbine; and second to provide a more detailed study of the changes introduced by the device in the pressure profiles on the roof of the house.

In order to measure the static pressure on the roof of the house, a series of 1 mm diameter holes were created on the roof. The entire house was 3D-printed using the MakerBot printer; and that allowed the dimensions of the holes and the distance between them to remain very accurate, thus yielding better results. **Error! Reference source not found.**32 shows the final roof printed. The small cylinders represent a guide that was added to each hole in order to fix the small hoses from the data acquisition unit in them.

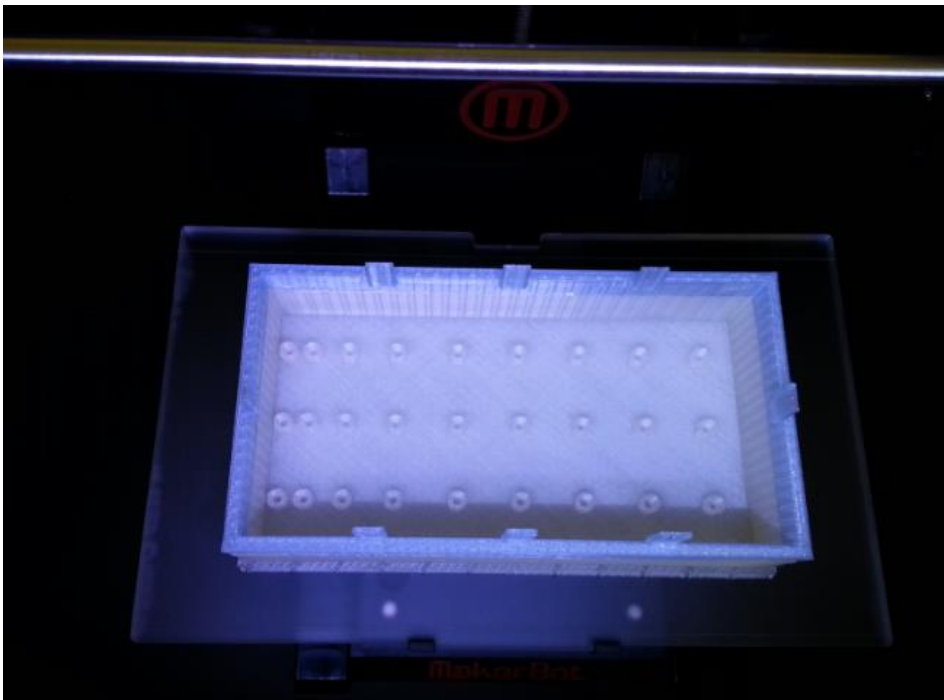


Figure 32: 3D-printed house roof



Figure 33: Roughness surface lecture

Since the 3D printing technology creates layers that are not as smooth, the roughness factor was measured and recorded using a Mitutoyo machine. **Error! Reference source not found.** shows the roughness measured for the roof of the house. This value for the roughness was later used as an input for the simulations.

A total of 9 hoses were installed in the roof. These hoses were connected to the data acquisition unit, which contains sensors that read pressure. These series of holes allow the reading of the static pressure in the roof of the rectangular house. **Error! Reference source not found.** and 35 show

the roof and DAU setup with the small hoses attached to them.

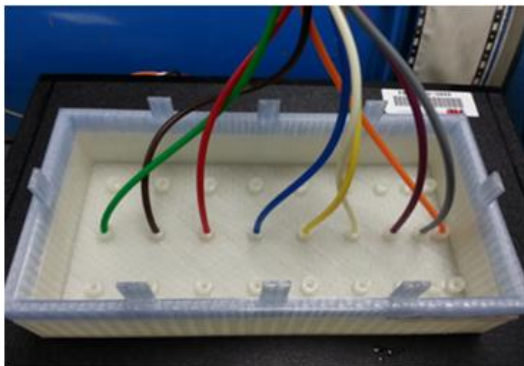


Figure 34: Roof setup for pressure reading



Figure 35: Data acquisition unit setup for pressure reading

Along with the static pressure in the roof, the angular velocity of the turbine was recorded. A digital tachometer was used to record each time that a blade went through the pointed location. This number was then divided by the number of blades to calculate the angular velocity of the turbine in RPM. The values in RPM were recorded 5 times each and then the average value was calculated. The calculated value was converted to radians per second, which is the unit that ANSYS takes as an input.



Figure 36. LINI-T 5URH0 digital tachometer

Finally, to complete the setup of the experiment a series of steps were carefully taken. First, the upper part of the wind tunnel was removed. The house was placed at the center of the section. The turbine was introduced through the top and then placed in the cross experimental section. The distance between the turbine and the house was measured with a caliper to maintain the X position discussed in the previous section of this report. The hoses were positioned at the end of the section, so that their interference with the flow patterns was minimal. Additionally, a video camera was placed about 3 meters from the wind tunnel to record the experiment. Figure 37. Three straight blades turbine,

experimental setup shows the final setup of the experiment. All experiments were performed twice, first for a wind speed of 8 meter per second, and then at 10 meter per second.

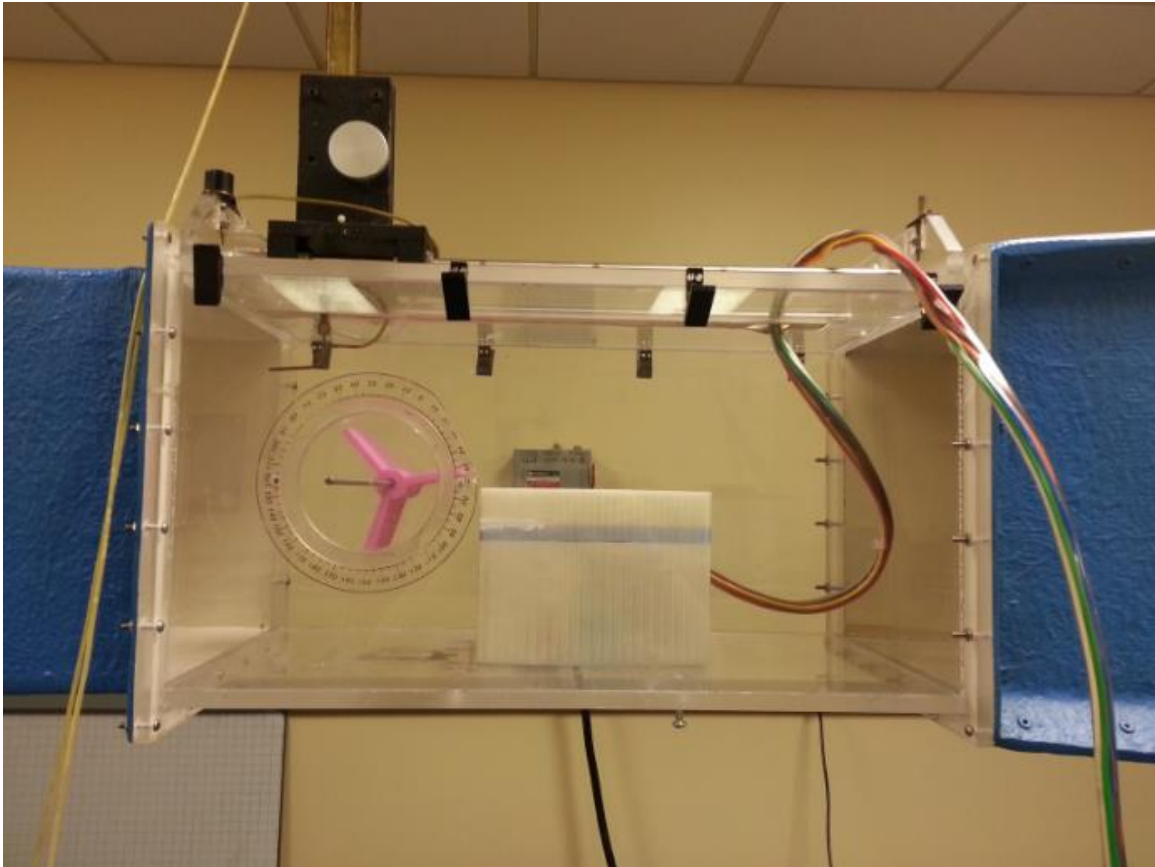


Figure 37. Three straight blades turbine, experimental setup

5.2.2 House

The experiment began with the analysis of the house alone. The same parameters used in the experiment were also declared in ANSYS and both results were compared in the figures below. Both graphs show that the pressure decreases with the wind speed and that the total pressure difference on the roof increases. This increase in the pressure difference

is known as uplift effect, and the mitigation of the same is one of the main objectives of this study.

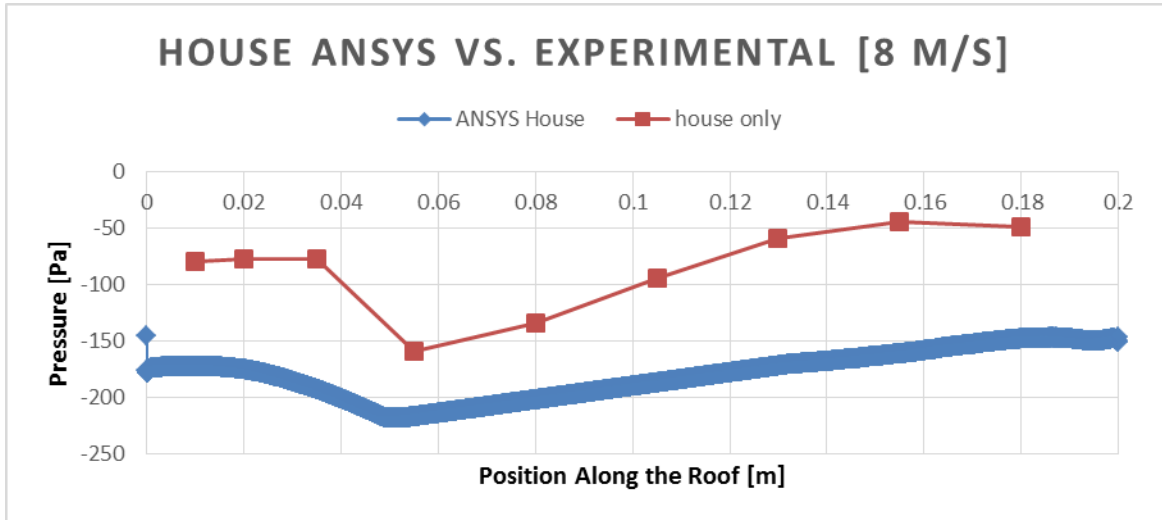


Figure 38. Static pressure house at 8m/s

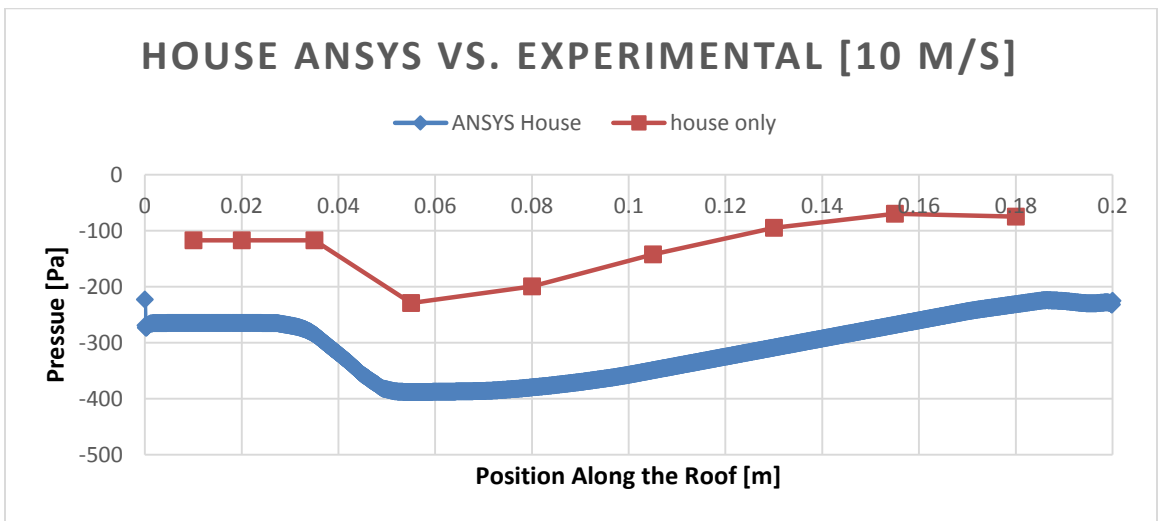


Figure 39. Static pressure house at 10m/s

All the devices designed in the following sections and their mitigation capabilities were compared to the previous two graphs.

5.2.3 Straight Blade

The preliminary ANSYS simulations showed that a high-pressure section occurred in the front wall below the turbine. As a result, the possibility of a rotation counterclockwise was expected. The counterclockwise rotation of the turbine generates a boundary layer separation increase, thus, generating an increment in the pressure difference on the roof of the house. In other words, this type of rotation increases the uplift effect rather than reducing it. The values of the static pressure recorded during this experiment were compared in a graph along with the values of the Static Pressure Plot extracted from the ANSYS simulations.

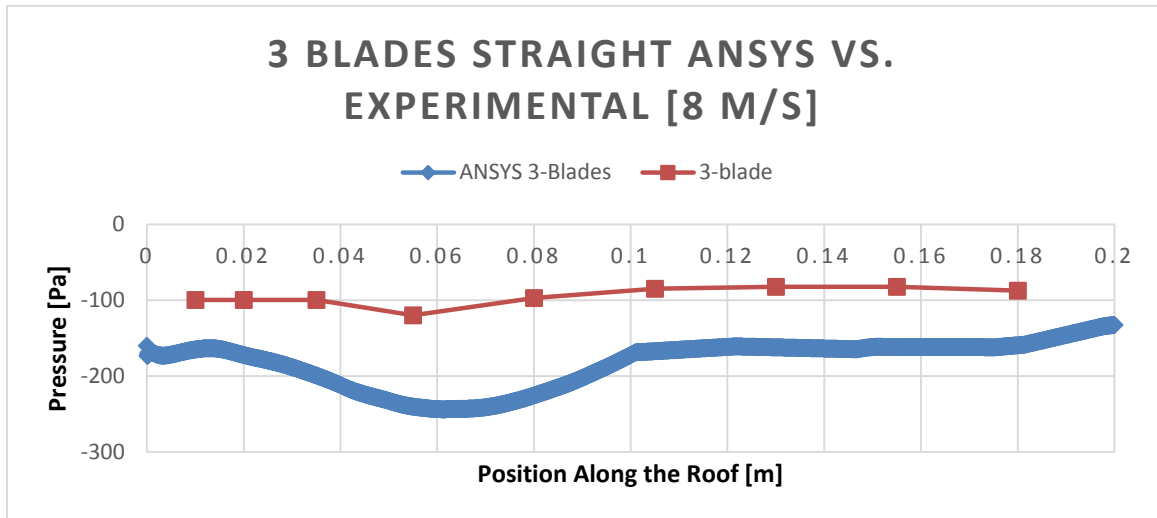


Figure 40. Static pressure 3 blades straight at 8m/s

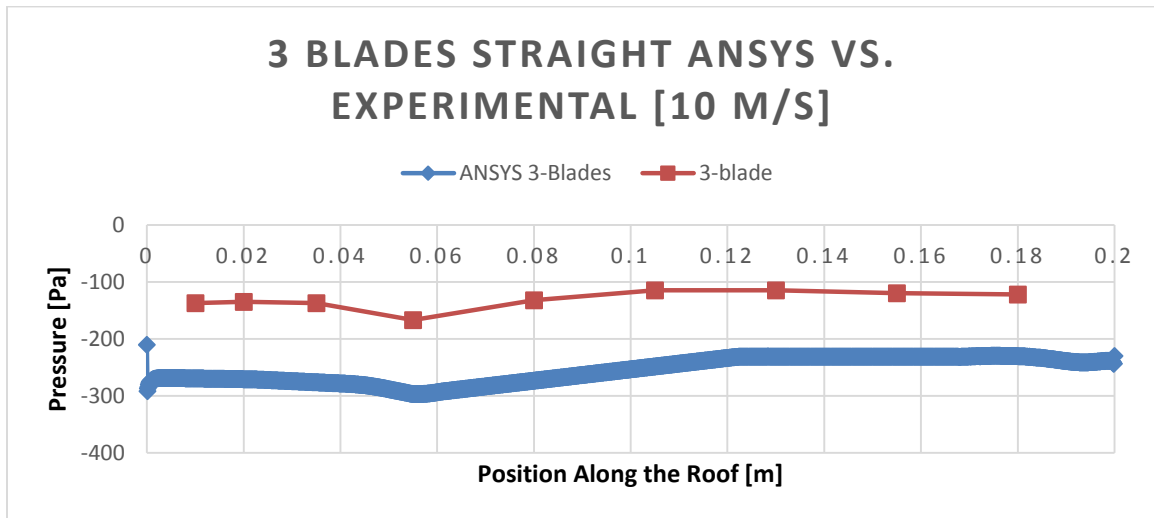


Figure 41. Static pressure 3 blades straight at 10m/s

This experiment showed that the 3 blades straight arm turbine did rotate in the counterclockwise direction; therefore, it is not desired and goes against the physical principle being pursued in this senior design project. As a design improvement step, an angle of twist was added to the 3-blade turbine to further study the wind mitigation with straight blade turbines.

5.2.4 Straight Blade Twisted

The angle of twist added to the turbine was selected based on having a final angle of twist of 180 degrees on the turbine; similar to a Windside turbine. Since the diameter was equal to the length on the prototypes built, the angle of twist was divided by 4 so that the real turbine would have a length of 4 times the diameter. In other words, the angle of twist on the prototypes was 45 degrees. The distance between the house and the turbine was maintained equal to the first experiment. The static pressure on the roof of the house

obtained in this experiment, for velocities of 8 m/s and 10 m/s, are shown below in Figure

42. Static pressure 3 blades twisted at 8m/s⁴² and 43 respectively.

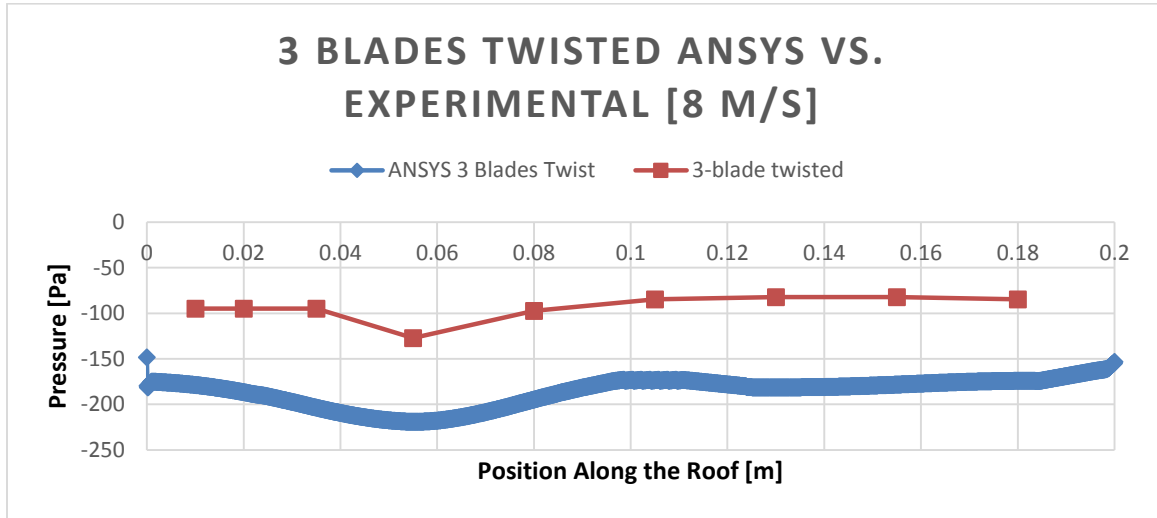


Figure 42. Static pressure 3 blades twisted at 8m/s

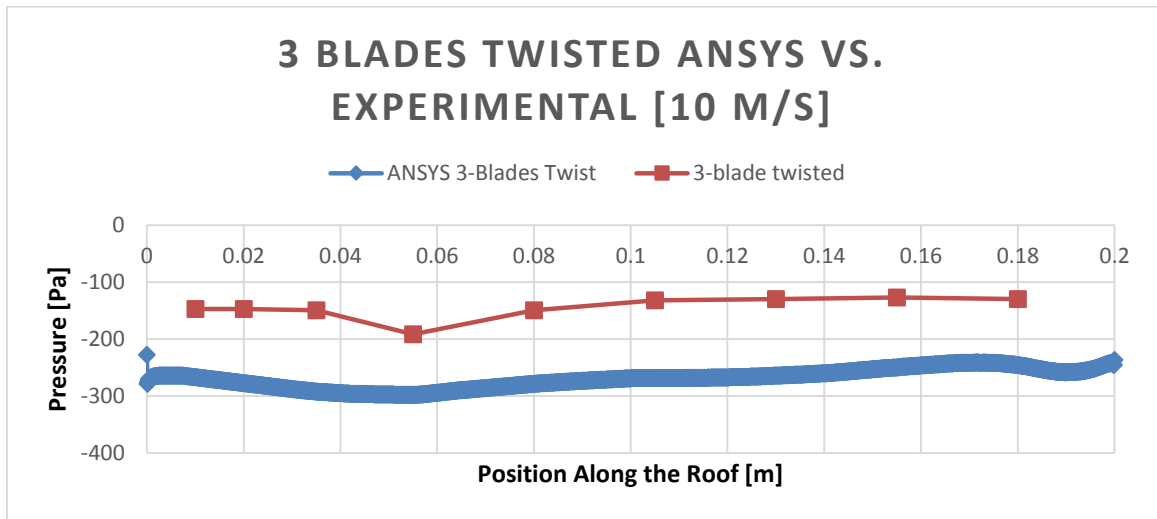


Figure 43. Static pressure 3 blades twisted at 10m/s

In this experiment, as expected, the twist did not produce a change in the rotation of the turbine. In other words, for this case the turbine still rotated in the counterclockwise direction; which was not desired. Additionally, the experiment showed that the mitigation

did not change by adding a twist on the turbine. However, the angular speed increased; and consequentially increased the power output.

Table 5. Angular speed of 3 blades with and without an angle of twist.

3-blade		3-blade twisted	
8 m/s	10 m/s	8 m/s	10 m/s
55.236	71.279	56.109	83.678

The first two experiments were performed using straight blade turbines, and the results showed that the rotation occurred only counterclockwise. This of course, is the result of the air impacting the front wall of the house and redirecting to the roof at very high speeds. As a result, a high pressure of air is generated in the lower part of the turbine producing the counterclockwise rotation. To avoid this type of rotation, a Savonius turbine was designed to replace the straight blade turbine, being studied up to this point. This new design represents the next design improvement in the progression study.

5.2.5 Two Blade Savonius

The two blade Savonius turbine was designed with a circular radius, and with a diameter equal to the tip-to-tip distance previously calculated. The turbine has two blades; it's closed at the center and has the same 45 degree angle of twist to ensure higher performance. The center hole has the same dimensions as the previous models and the same type of bearing and shaft were used in the experiment.

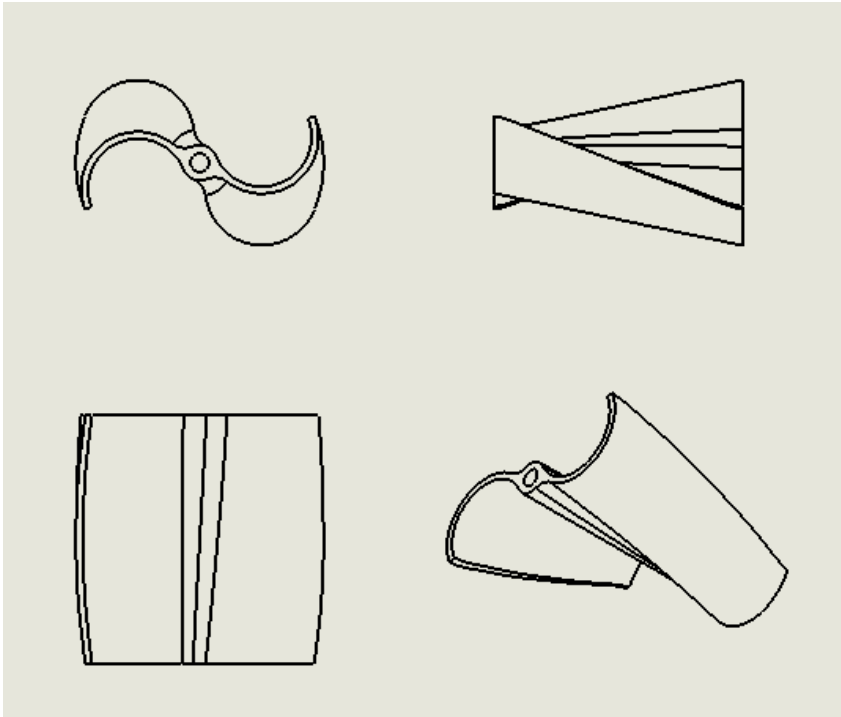


Figure 44. Two-blades Savonius turbine

The following figures show a comparison between the static pressure measured during the experiment and the ANSYS simulation.

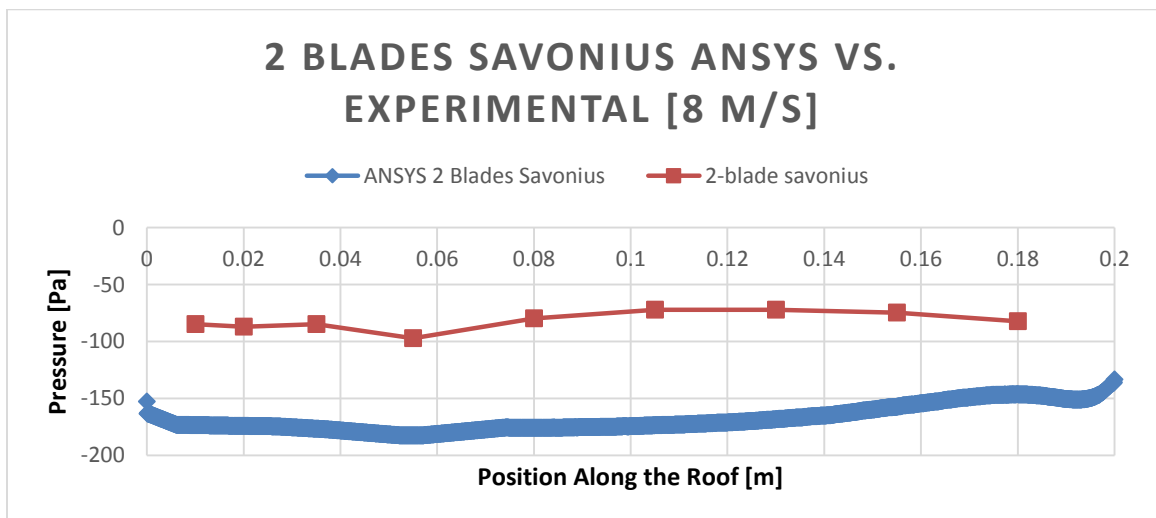


Figure 45. Static pressure 2 blades Savonius at 8m/s

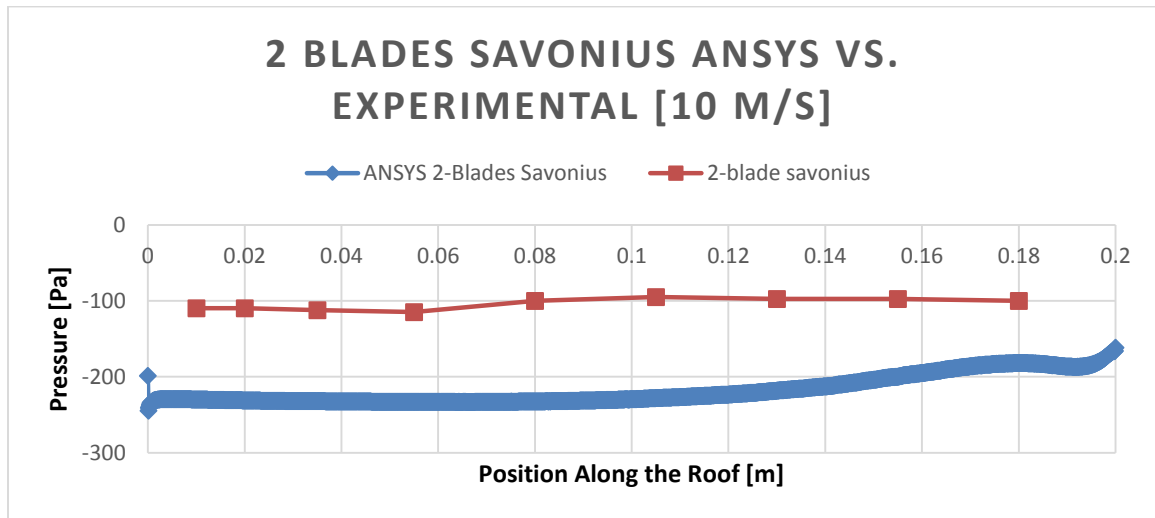


Figure 46. Static pressure 2 blades Savonius at 10m/s

The pressure difference on the roof is clearly smaller than those obtained with the straight blade turbines. As expected, the turbine rotation was clockwise, which is directly related to the mitigation obtained. However, during the experiment, the turbine stopped on a semi-horizontal position for a few seconds as the air velocity changed from 3 to 7 meter per second. This means that this device requires velocities higher than average to be functional because it requires a higher speed to start rotating. It is valid to mention that the angle of twist of 45 degrees was the main cause for this. In the presence of a longer turbine with a complete 180 degrees twist, smaller velocities may start rotation. As a result of this experiment, a three and four blade Savonius were also studied.

5.2.6 Three and Four Blade Savonius

The 3 blade Savonius has the same blade shape as the 2 blades. The same type of shaft and bearings were used and the study was also made at 8 and 10 meter per second. The static pressure on the roof is shown in the following two graphs.

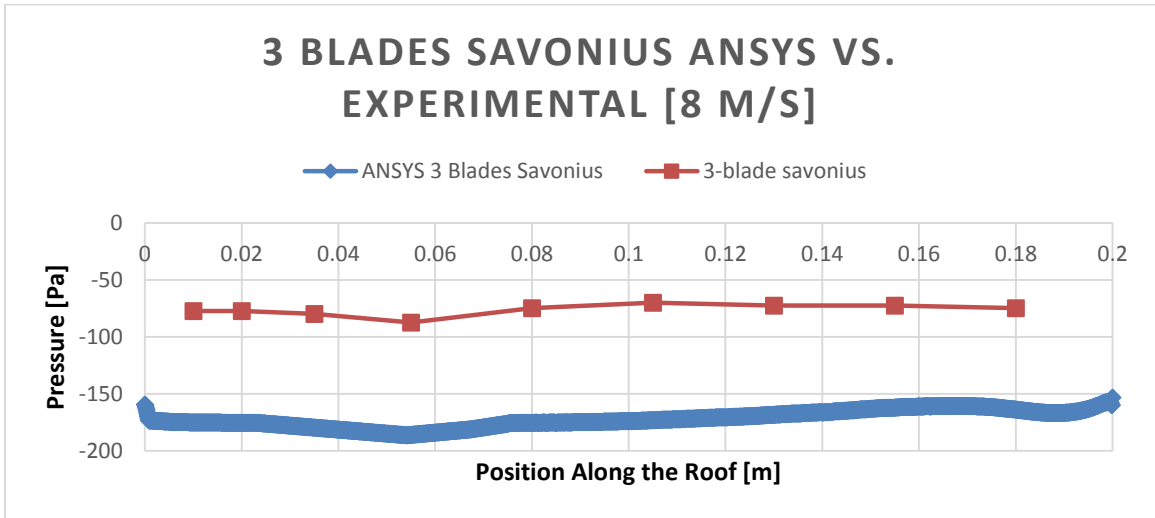


Figure 47. Static pressure 3 blades Savonius at 8m/s

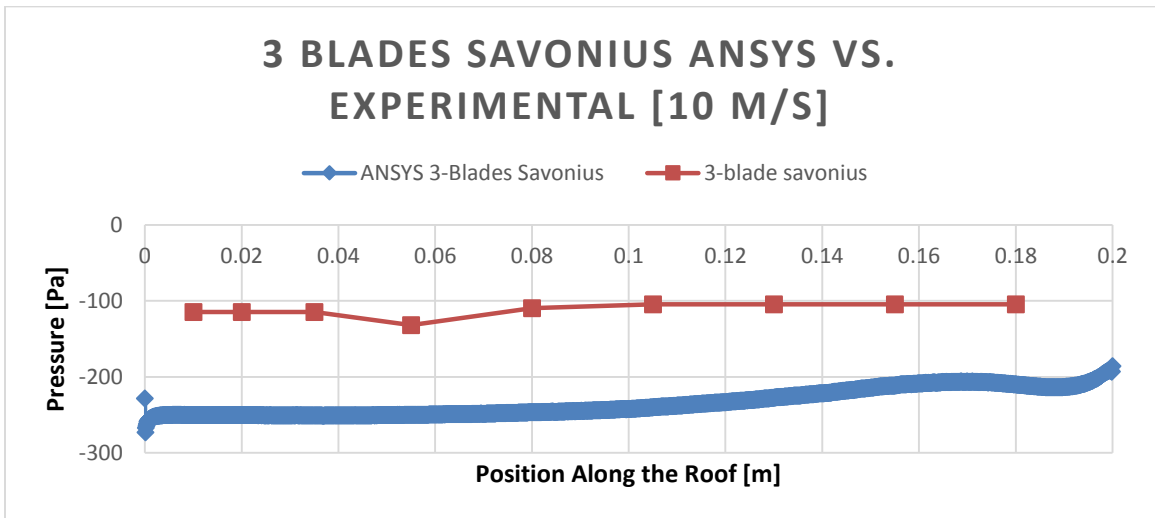


Figure 48. Static pressure 3 blades Savonius at 10m/s

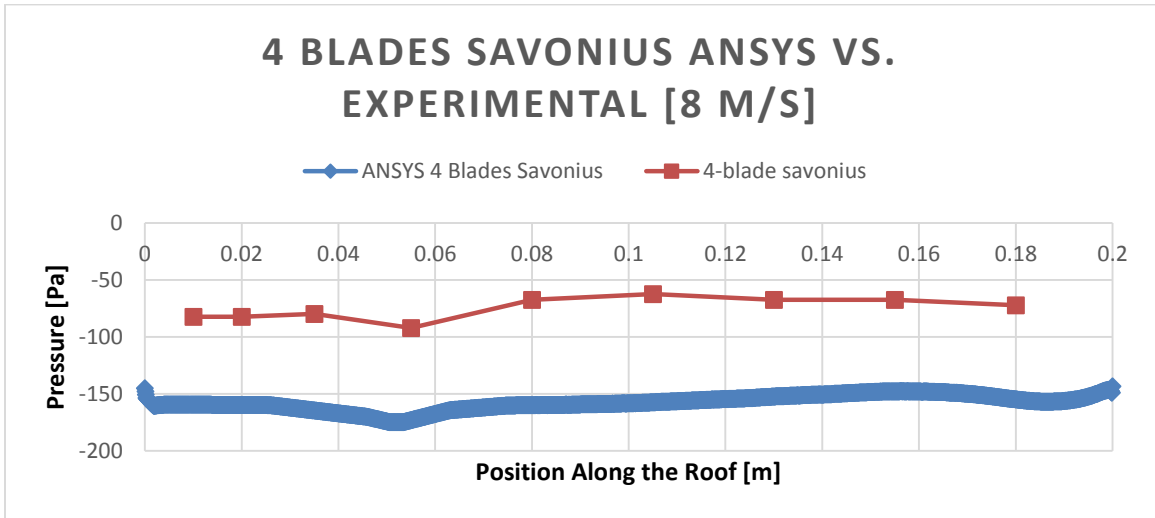


Figure 49. Static pressure 4 blades Savonius at 8m/s

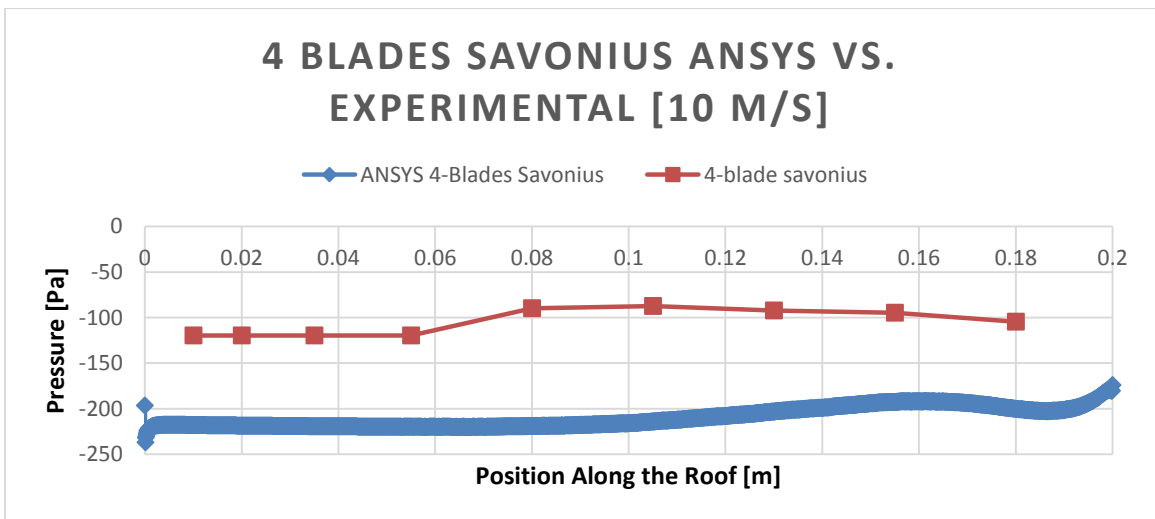


Figure 50. Static pressure 4 blades Savonius at 10m/s

As can be seen in Figure 47. Static pressure 3 blades Savonius at 8m/s⁴⁷ and ⁴⁸, the mitigation obtained from the 3 blade Savonius is superior to that obtained from the previous 3 prototypes. However, Figure 49. Static pressure 4 blades Savonius at 8m/s⁹ and ⁵⁰ show that the four blade Savonius greatly reduces the pressure difference on the roof. Nevertheless, the 4 Blade Savonius had a significantly smaller angular velocity in

comparison to the 3 Blade Savonius. Table 6: Angular speed of 2, 3 and 4 blades Savonius. displays the angular velocities for the 3 Savonius turbines analyzed during the experiments.

Table 6: Angular speed of 2, 3 and 4 blades Savonius.

2-blade Savonius		3-blade Savonius		4-blade Savonius	
8 m/s	10 m/s	8 m/s	10 m/s	8 m/s	10 m/s
48.066	90.823	98.800	131.074	61.298	69.696

Based on the experimental results and the ANSYS simulations, the 3 Blades Savonius with an angle of twist of 45 degrees produced the best results in terms of wind mitigation and power generation combined.

5.2.7 Discussion

After analyzing all the data presented above, there are a few points that need some clarification. There is a noticeable difference between the results obtained from the experiment, and the results obtained from the simulation. Even though the curves present a very similar behavior, their magnitudes are a little far from each other. Some of the reasons that could have led to these differences are explained below.

First of all, it is important to note that all the simulation were performed using a 2D configuration. This configuration was chosen based on the lack of computing resources available to the team at the time of the analysis. Thus, this may have been one of the reasons that led to the aforementioned difference between the two. One of the factors that could have influenced this difference is the fact that a twisted turbine can redirect the air in three different directions. A two dimensional simulation does not accounts for other directions other than the two dimensions contained in the plane of the configuration. Nevertheless, to

prove the validity of the new concept device that is the purpose of this thesis, the behavior of the pressure distribution on the roof has a much stronger meaning than the magnitude of the values.

Another important factor to consider is the surface of the roof built for the experiment. This roof was printed using the MakerBot Replicator 2, whose specifications are explained in section 5.2.1. In addition, the patterns of the layers on the roof are not aligned with the direction of the flow as shown in Figure 51 below. This could have caused the wind to be redirected along these lines, which could have also been responsible for altering the pressure readings.

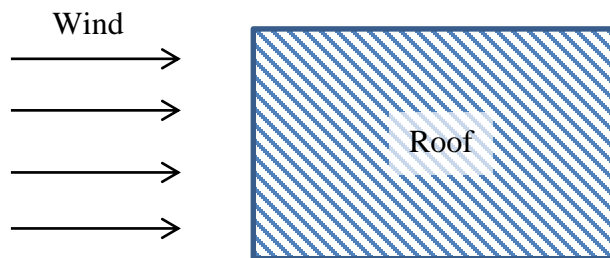


Figure 51: 3D printed roof, pattern of the layers

5.3 Proposed Design

In order to determine which design is the best possible among those studied, a series of factors were considered. To accomplish that goal, it is important to look at the following graphs, which show all the turbines together in one single chart.

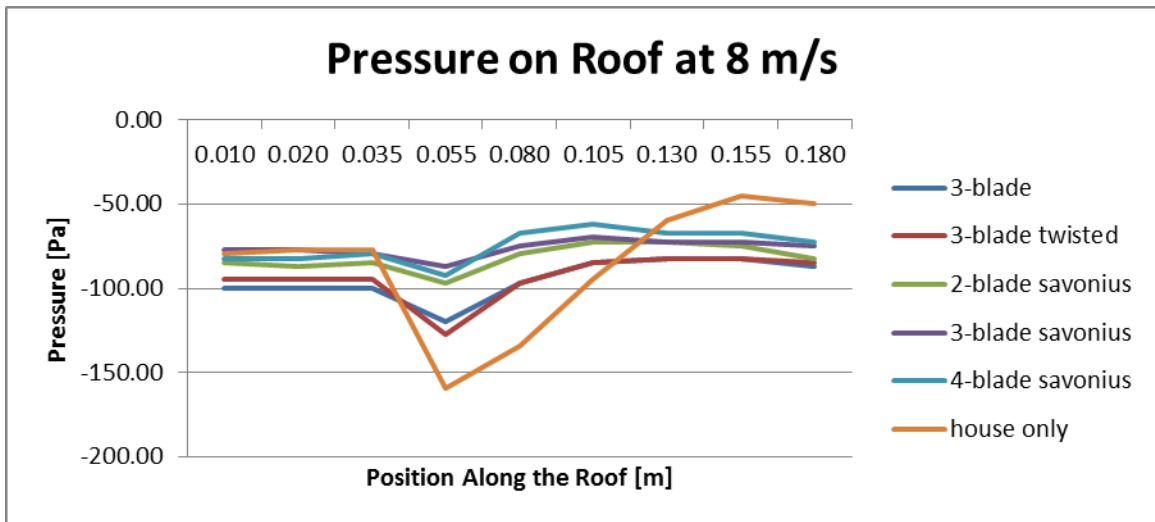


Figure 52: Pressure profile over roof for 8 m/s velocity

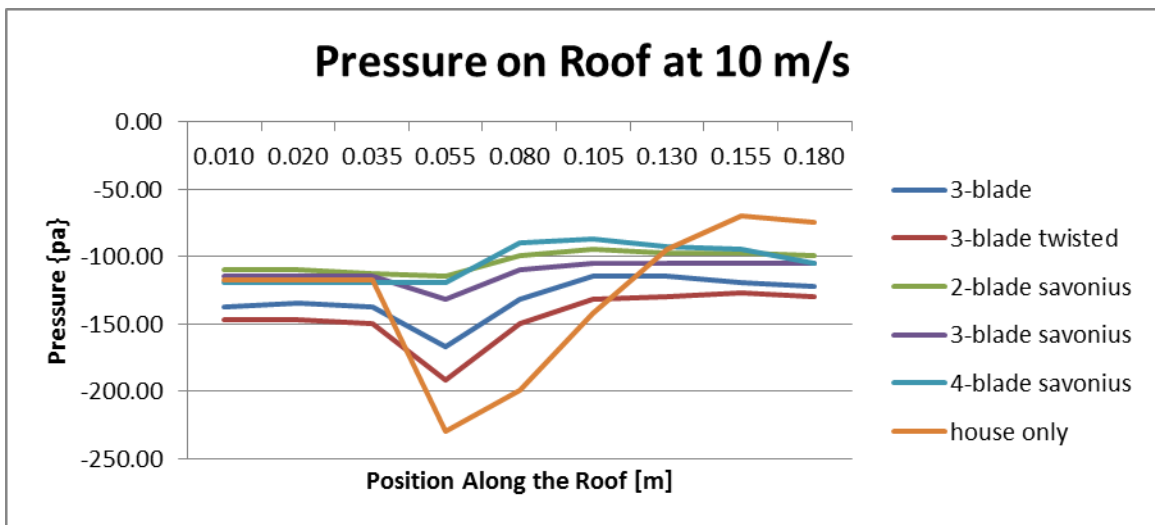


Figure 53: Pressure profile over roof for 10 m/s velocity

First of all, it is important to note the distribution of pressure over the roof, which is similar for 8 and 10 m/s velocities. As the graphs suggest, positioning any of the devices in front of the house has a significant impact on the pressure distribution. It can be observed how the lines are much smoother with any of the devices when compared to the house alone. In other words, when the house is alone the pressure starts at a certain value, and

then plummets towards a very negative value. This could be translated into a vacuum effect in a real situation. This sudden change in pressure produces very high forces and torques on the roof, thus producing a very significant uplift. On the other hand, when the devices are placed in front of the house, the vacuum is reduced thus reducing the force on the roof. Also, and most importantly, the sudden changes are eliminated, thus dramatically reducing the high torques and consequently the uplift loads.

A second consideration is of course the values of the pressure along the roof of the house. It is clear that any of the devices somehow improves the pressure on the roof. However, it is clear that the 4-blade Savonius yields the best results in terms of reducing the uplift force; thus this would be the best pick based solely on that criterion. However, it is also important to consider manufacturability issues, and for that reason the other two Savonius models come into play. First of all, the 4-blade Savonius costs approximately $\frac{1}{4}$ more than the 3-blade, and close to $\frac{1}{2}$ more than the 2-blade. Therefore, for manufacturability considerations the 4-blade Savonius becomes less preferable. Furthermore, if rotational speed is considered as well, which is one of the most important factors for power generation, the 3-blade version is by far the most suited when compared to the 2 and 4-blade. In conclusion, based on an overall assessment that involves uplift mitigation, power generation, and manufacturability, the recommended choice becomes the 3-blade Savonius.

6. ESTIMATIONS FOR PROTOTYPE

From this point on, the 3-blade Savonius has been chosen as the best design among those studied; therefore all the following analysis is based on that particular turbine. This

section is dedicated to perform estimations of the real life device based on all data previously obtained.

As a first step, the rotational speed of the actual size device is estimated using dimensionless numbers. It is important to estimate the rotational speed because it is used to calculate the power, which is then used to find the torque provided by the device. This torque is then used to select an appropriate generator to produce electricity.

6.1 Dimensionless analysis for power generation

Given the limited data obtained from experiments and simulations, an estimation of a real size situation was performed assuming the following conditions:

1. Temperature of the fluid is constant because the model and prototype have similar working environment.
2. Constant wind speed was assumed. The purpose behind this condition was to use the same air velocity for both the model and the prototype, thus being able to use some of the dimensionless numbers to analyze other variables. In other words, the analysis involves determining what would happen if both the model and the prototype were placed side by side in a test area of actual house.
3. Constant density of air was also assumed, given temperature is a constant.

The initial step towards real-life estimation is to obtain the speed of rotation of the real size device. For this, Reynolds number was used. Since the rotational speed of the models are known from experiment, these speeds can be used to estimate those of the real size

device. The following table shows the rotational speeds of the 3-blade Savonius model obtained from experiment:

Table 7: Experimental angular velocity at different wind speeds for 3-blade Savonius model

Air Speed [m/s]	Angular Velocity of Model [rad/s]
3	30.983
4	40.226
5	49.086
6	59.732
7	71.405
8	98.8
10	31.074

Reynolds number follows this relation:

$$Re = \frac{\text{inertial forces}}{\text{viscous forces}} = \frac{\rho V D}{\mu}$$

With density, velocity, and viscosity being the same for both the model and prototype, the only value relating both was the diameter. This led to the following relation:

$$D_{model} = D_{prototype}$$

Obviously this relation has no meaning because the diameters of the prototype and the model cannot be equal. Thus, a different dimensionless number was considered.

The next step was to consider Mach number. The main objective with using this dimensionless number was to calculate the rotational velocity of the real size model, thus being able to estimate power generation capabilities. Therefore, the following relation can be established:

$$M_{model} = M_{prototype}$$

Where,

$$M = \frac{V}{c}$$

Substituting the first relation above gives:

$$\left(\frac{V}{c}\right)_{model} = \left(\frac{V}{c}\right)_{prototype}$$

Given that the speed of sound is a function of temperature, it does not change because temperature is constant. Thus, the following relation can be derived:

$$V_{model} = V_{prototype}$$

Now rewriting the same in terms of angular velocities it follows that:

$$(wr)_{model} = (wr)_{prototype}$$

Thus, since the purpose of this analysis is to obtain the rotational speed of the real size prototype, the above equation can be solved for this value as follows:

$$w_{prototype} = \frac{w_{model} \cdot r_{model}}{r_{prototype}}$$

Using a diameter of 0.5 m and 0.123 m for the prototype and model respectively, the angular velocity for the prototype was obtained. The following table shows the rotational speeds of the real size 3-blade Savonius prototype at different wind speeds, the table was constructed using the relationship shown above.

Table 8: Angular velocity at different wind speeds for 3-blade Savonius real-size turbine

Air Speed [m/s]	Angular Velocity of Prototype [rad/s]
3	7.55
4	9.81
5	11.97
6	14.57
7	17.41
8	24.09
10	31.96

Once the rotational speed values were obtained, the power and torque output could be calculated. In order to calculate those values, some other variables were necessary. All the equations used to arrive to the results are explained in more detail in sections 3.2 and 3.3. The following chart shows the results for the estimated output power and torque of the prototype:

Table 9: Torque and power calculations for prototype

Air Speed [m/s]	Turbine Angular Velocity [rad/s]	TSR	Power Coefficient, Cp	Power Output [W]	Output Torque [N-m]
3	7.55	1.259	0.2623	3.4063	0.4509
4	9.81	1.226	0.2722	8.3796	0.8543
5	11.97	1.197	0.2803	16.8555	1.4083
6	14.57	1.214	0.2759	28.6655	1.9681
7	17.41	1.244	0.2669	44.0389	2.5293
8	24.09	1.506	0.1566	38.5640	1.6008
10	31.074	1.598	0.1012	48.6673	1.5662

The table also shows the calculated values for the tip speed ratio, TSR, and the power coefficient, Cp. The TSR is a function of both the rotor speed and the air speed, while the Cp was obtained as a function of TSR from Figure 10. If the curve pertaining to a Savonius rotor in Figure 10 is closely analyzed, it can be seen that these kinds of turbines reach a

maximum of $C_p = 0.34$. This maximum value of C_p corresponds to a TSR of less than one, and represents the maximum possible efficiency of such a device. Thus, it makes sense that the values for the prototype being analyzed here be lower than those maximum values, since the TSR values obtained are higher than unity. This means that the efficiency of the turbine presented here is lower than the possible maximum, as seen by looking at the smaller values of C_p obtained in the chart. Nevertheless, it is important to consider that the values obtained in Table 9 were calculated based on an almost frictionless motion of the device. This means that once the device is attached to the electric generator, the rotor should rotate slower due to the back torque exerted by the generator. Consequently, this can be translated into a lower TSR, which automatically increases the efficiency of the device according to the curve shown in Figure 10.

6.2 Other Considerations: Electrical Setup

In order for a wind turbine to produce useful energy, it has to be connected to a series of electronic components that are designed to transform the rotational mechanical energy produced by the turbine into useful electrical energy. In other words, the turbine transforms the kinetic energy carried by the wind into rotational energy, and this rotational energy is further transformed into electrical energy that can be used to power any home device or appliance, etc. These electronic components include generators, converters, inverters, etc.

An electric generator is basically a device that converts mechanical energy into electrical energy. There are many different kinds of generators that are commonly used with wind power generation. Some examples include induction, synchronous, and

permanent magnet generators, etc. (Goudarzi & Zhu, 2013). Induction generators were first introduced for fixed speed, and later improved to generate power under variable speeds of operation. These types of generators usually include gearboxes and components that require regular maintenance. Also, they require expensive equipment in order to connect them to the grid. Synchronous generators are also available for fixed and variable speeds of operation of the wind turbine. Finally, permanent magnet generators are among the most widely used. In these kinds of generators, the rotor is replaced with a permanent magnet, which provides the excitation explained by Faraday in his explanation of the induction through magnetic flux variations (Goudarzi & Zhu, 2013).

An electric power converter is a device that converts electric power from one form to another, which means they can convert from DC to AC current, or vice versa. Furthermore, converters can also change the voltage or the frequency of a signal. These types of electronic devices may be composed solely of electric devices such as diodes and resistors, etc., or they may also be composed of a combination of mechanical and electrical components. Different arrangements of these components result in a different purpose, as described above.

An electric inverter is one type of converter. An inverter takes a direct current signal and converts it to alternating current; in other words, an inverter transforms DC to AC. This conversion may be achieved by using a combination of switches and transformers in the form of windings (MITOpenCourse, 2007).

Many of the large scale wind turbines nowadays use AC generators because these turbines have mechanism that keeps them turning at a constant speed. Large size wind

turbines can generate a very large amount of useful power. For example, the Enercon E126 can generate as much as 7.5 MW. Some of the leading manufacturers of such large turbines include Samsung, Siemens, Vestas, and GE Power, among others.

For small scale turbines, it is better to use DC generators which generate direct current at different rotational speeds. Permanent magnet generators are among the most commonly used because of their efficiency in extracting the power from the mechanical work provided by the turbine. Furthermore, permanent magnet generators are simple and economical to manufacture and maintain.

It is also important to determine if a gearbox is necessary to increase the rotational speed. Some electric generators require a higher rotational speed than the one provided by the turbine, thus a gearbox is required. Some of the commercially available wind turbines include gearboxes; one such example is the Jacobs 31-20 from Wind Turbine Industries Corporation (Wind Turbine Industries Corp.) On the other hand, there are some direct drive generators which are directly connected to the rotor of the turbine. The advantage of gear drive machines is that they can produce more power at a lower cost than direct drive machines. The disadvantage is that gearboxes include many moving parts that require more maintenance (Sagrillo, 2002).

For the present project two different alternatives were considered, these two options are discussed below.

6.2.1 Electrical Setup Alternative 1: House Grid Connected System

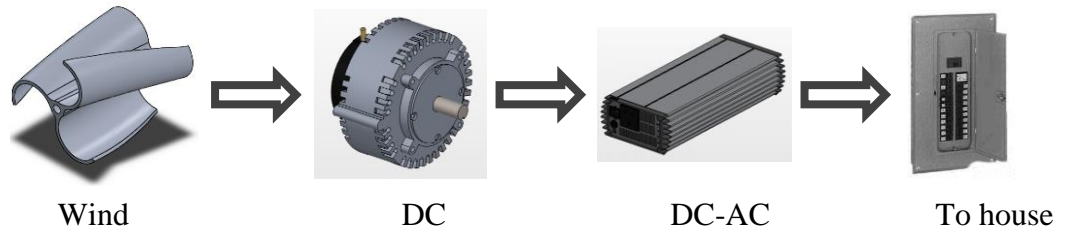


Figure 54: Electrical setup alternative 1

The first alternative being considered is shown in Figure 54: Electrical setup alternative 154. This alternative proposes a direct drive generator connected to the turbine, followed by an electric inverter. The purpose of the inverter here is to convert the DC provided by the generator into usable alternating current that could be supplied to the electric grid of the house.

6.2.2 Electrical Setup Alternative 2: House Grid Connected System with Storage

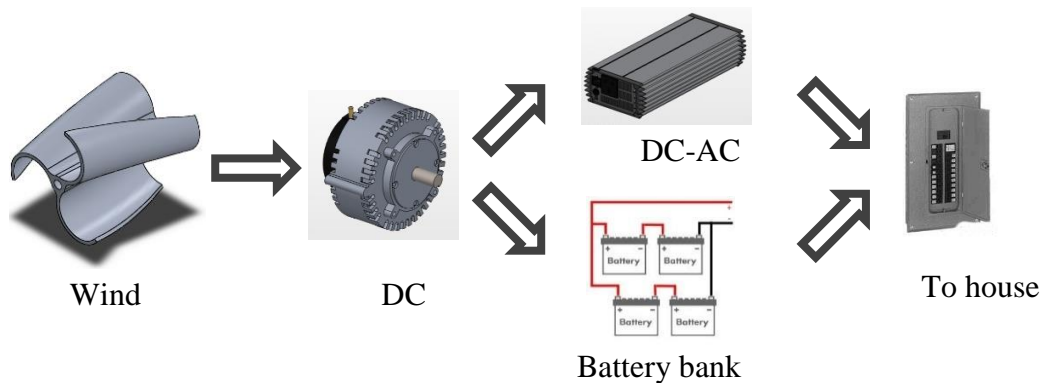


Figure 55: Electrical setup alternative 2

With the setup in Figure 55: Electrical setup alternative 255, the energy provided by the wind turbine can be better utilized compared to alternative 1. With a bank of batteries available, even when the wind is not strong enough, the system can still store this small amount of energy into the batteries for later use.

6.2.3 Electrical Setup Alternative 3: Power Provider Grid-Connected System

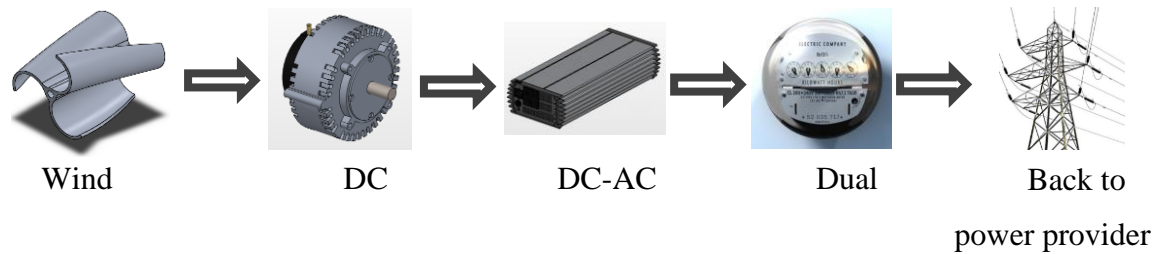


Figure 56: Electrical setup alternative 3

The alternative in Figure 56: Electrical setup alternative 3 is suited for a system that has a good source of wind available. When the system is providing more electricity than needed for regular consumption, this surplus can be “sold” back to the provider by means of a dual meter. A dual meter allows electricity to flow in both directions, and at the end of the establish time period it calculates the net power to determine if the house should either pay, or receive money for the given period.

6.2.4 Feasibility Assessment

While all three alternatives are feasible, when it is time to choose the right choice, it is up to the customer to decide. However, there are a few pros and cons for each of the above discussed alternatives that could help making a decision.

The first alternative offers the easiest solution. It is the most economical because it contains the least amount of electronic components. However, production is limited to factors such as available wind, size of the turbine, and consumption. With this arrangement, if wind is not present, the system does not provide any energy. Thus the homeowner needs to be connected to the electric company grid for situations like this.

The second alternative offers a more useful arrangement. The batteries allow the owner to store energy when it is not needed, or when it is not enough to power the house grid. In other words, if the system is producing more energy than needed, the extra energy can be stored. Furthermore, when the system is producing electricity, but it is not enough to power the house, this little energy can still be stored. This alternative is a little more costly, but it is the best one for houses located where no utilities are available. With this arrangement, provided there is enough wind energy, the system can be generating electricity to power the entire house and charging the batteries at the same time. While there is wind the system can be directly connected to the house grid, and when the wind is gone, the batteries should provide the energy.

The last alternative is ideal for systems that have a large amount of wind energy available. With this arrangement, the owner can provide electric power to the house as well as to the electric company. In other words, the owner can “sell” the extra energy back to the power company.

7. COST ANALYSIS

7.1 First Prototype

The following table shows the cost analysis for the construction of the first prototype presented in section 4 of the present report.

Table 10. Prototype cost analysis

Item	Unit Price	Quantity	Subtotal	Source
Balsa wood sheet	\$14.00	5	\$70.00	Michaels Stores
Crazy glue	\$7.50	1	\$7.50	Michaels Stores
Wood shaft	\$15.00	1	\$15.00	Michaels Stores
Sand paper	\$4.00	5	\$20.00	Michaels Stores
Wood square sticks	\$2.00	10	\$20.00	Michaels Stores
Wood shaft	\$8.00	1	\$8.00	Michaels Stores
		TOTAL	\$140.50	

7.2 Experiment Parts and Equipment

As mentioned before, there were 5 different models used for experiments at the wind tunnel. These models were 3D-printed using the MakerBot Replicator 2. Also, 3 steel shafts and 6 ball bearings were used as explained in section 5.2.1. The following chart summarizes all cost incurred for experiments:

Table 11: Cost of experimental parts and equipment

Item	Unit Price	Quantity	Subtotal	Source
3D Printer MakerBot Replicator 2	\$2,100.00	1	\$2,100.00	Microsoft Store
3D printer replacement cartridge	\$48.00	1	\$48.00	Microsoft Store
Bearings (PN: 57155K352)	\$6.10	6	\$36.60	McMaster Carr
Miniature drive shaft (PN 1327K54)	\$9.59	3	\$28.77	McMaster Carr

TOTAL	\$2,213.37
--------------	-------------------

7.3 Prototype

The cost of the prototype could not be determined exactly because it was not actually built. All the numbers in this section correspond to price quotes obtained from the Manufacturing Process Lab at FIU, more specifically from Mr. Richard Zicarelli, who is the professor in charge of this facility.

12: Estimated cost of prototype

Item	Unit Price	Quantity	Subtotal	Source
Parts				
Shaft (PN: T434)	\$81.36	1	\$81.36	Metals Depot
Aluminum Sheets (PN: S3050)	\$115.20	2	\$230.40	Metals Depot
Square Bars (PN: SQ4316)	\$18.60	1	\$18.60	Metals Depot
Bearings (PN: 6384K373)	\$19.90	2	\$39.80	McMaster Carr
Labor				
Manufacturing: rolling, cutting, twisting, etc.			\$1,500.00	FIU Manufacturing Lab
Assembly and Attaching			\$700.00	FIU Manufacturing Lab
TOTAL			\$2,570.16	

7.4 Electrical System for Prototype

The cost of the electrical system depends on the customer needs. There is a wide range of options to choose from when it comes to DC generators and other components. For example, Windstream Power LLC has a series of generators available for purchase ranging from \$175 to \$525. These generators take a rotational motion as an input, and their output is based on the input torque. Each of these generators produces energy, some at low speeds, and the more expensive ones at higher speeds. Therefore, the best choice

completely depends upon the available wind energy at the location where the turbine is installed. Some of the available manufacturers of electric components specializing in wind power include Windstream, Alxion, Polar Power, Wind Blue Power, among others. Prices of generators range from \$180 to \$600 for larger generators. Prices vary according to maximum current output. The other components can also be purchase from some of these manufacturers, and prices range from \$100 to around \$500 as well.

8. TIMELINE AND RESPONSIBILITIES

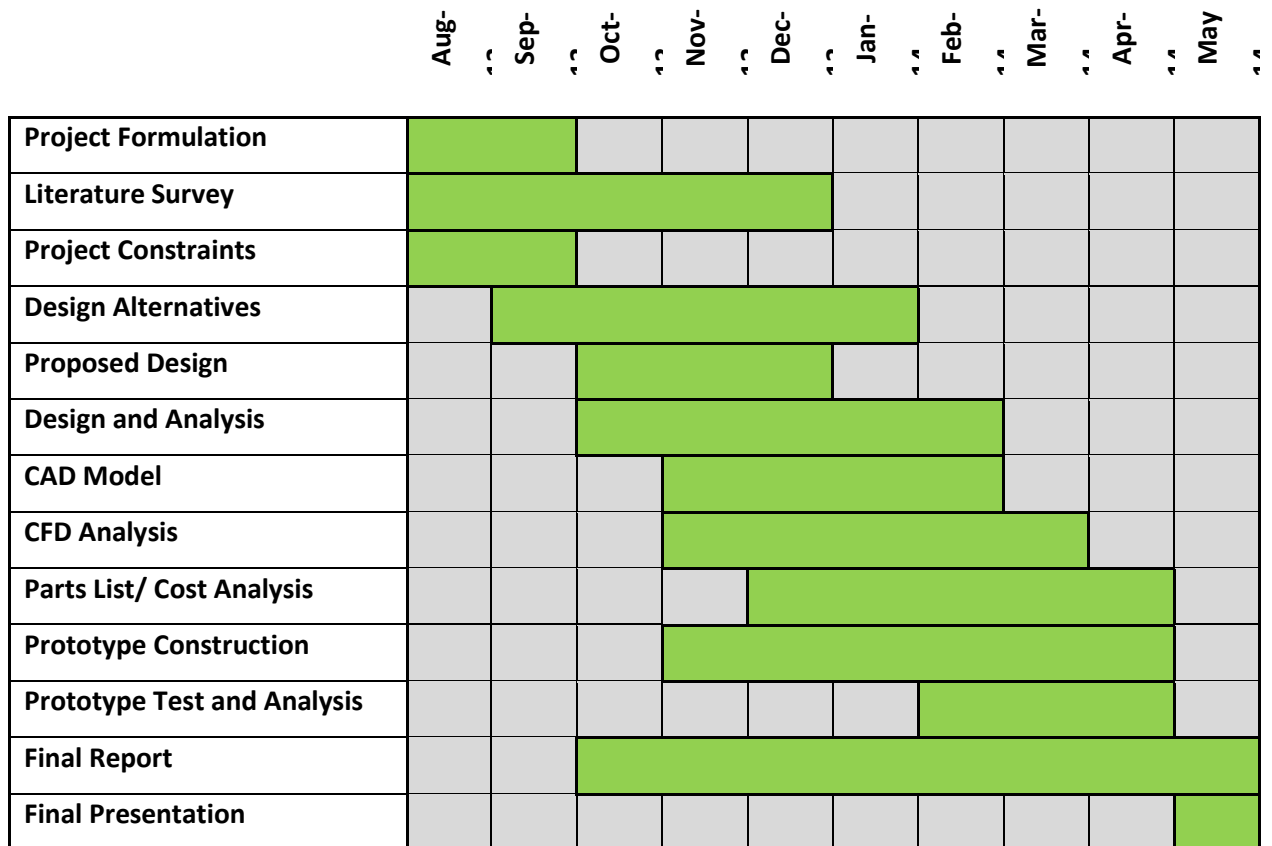


Figure 57: Timeline

	Team Member(s) Responsible
Project Formulation	Yoel
Literature Survey	Marcos
Project Constraints	Marcos, Yoel, Yunior
Design Alternatives	Yoel, Yunior
Proposed Design	Yoel, Yunior
Design and Analysis	Marcos, Yoel, Yunior
CAD Model	Yunior
CFD Analysis	Marcos, Yoel, Yunior
Parts List/ Cost Analysis	Marcos, Yunior
Prototype Construction	Yunior, Yoel
Prototype Test and Analysis	Marcos, Yoel, Yunior
Final Report	Marcos, Yoel, Yunior
Final Presentation	Marcos, Yoel, Yunior

Figure 58. Team responsibilities

9. CONCLUSIONS

This Senior Design Project pursued the creation of a device that reduces the uplift effect on a conventional flat roof building while generating power. The mitigation was achieved through the modification of the boundary layer on the roof of the houses. The same was thoroughly studied through ANSYS Fluent and the results were correlated through experiments. The correlation was accomplished by setting a house setup with a series of

static pressure sensors to measure the values. The same boundary conditions were defined in ANSYS Fluent. The ANSYS Fluent procedure was established and described in a step by step manner with the purpose of defining a method of analysis for rotating wind mitigation devices. A mesh study was also made in order to obtain the best possible results. The values of the experimental and simulations were compared.

The correlation of results demonstrated that ANSYS Fluent 2D analysis can be used to predict the pressure profile on a roof with a rotating device before it. However, the pressure values can be estimated, but the results should be correlated with experimental results because the values may vary due to the nature of the 2D study.

Following the same method of analysis, the position in relation to the roof and the number of blades of the device were studied and defined. The analysis also demonstrated that the rotation of the device affect the wind mitigation. Similar to a rotating cylinder, the rotation of the device on a clockwise direction mitigate while in a counterclockwise it increases the boundary layer effect decreasing the pressure even though it “linearizes” the pressure distribution on the roof. This effect is also directly related to the shape of the turbine.

In conclusion, the study predicts that a 3 blade Savonius turbine with a diameter of 0.5 meters, a length of 2 meters, and an angle of twist of 180 degrees reduces the pressure difference in the roof by about 80 percent. Simultaneously, the device provides a power generation of at least 44 Watts, while the turbine peak efficiency is around 30 percent.

Although one of the main objectives of this Senior Design Project was to analyze winds between 2 and 32.5 meters per second, it was not possible because of the speed limitations

of the available wind tunnel. Nonetheless, the results obtained at 10 meters per second suggest that the mitigation capability of the device increases as the power generation efficiency decreases.

10. RECOMMENDATIONS

This project represents the very first step towards a new technology that had never been studied before. For that reason, there is still a long way to go from here to make this idea more efficient, more useful, and more affordable for the consumer. Due mainly to time constraints, there were many variables that were not considered for this initial study. Based on the experience collected by the team during this project, here are some recommendations for future development of this idea.

First of all, there are some design variables that should be further considered to improve the design of the model. One of those variables is the angle of twist of the turbine. The angle of twist represents a very important factor to consider because it can change considerably the power generation capabilities of the turbine, as well as the wind mitigation ability. It is recommended that experiments similar to those performed in this project be completed to find the optimal angle of twist of the turbine. Another design variable to consider in future studies is the shape of the blades. Finally, the shape of the blade is one design factor that consumes great amounts of computing resources, which were not available to the team at the time of the present study. It is recommended that available software is utilized to find an optimal shape for the blades taking into consideration lift and drag coefficients, as well as feasibility and manufacturability of the design.

For any system, it is extremely important to take into consideration the efficiency. Therefore, a critical step when manufacturing the prototype is to ensure it is well balanced; otherwise, the system capabilities might be compromised. An unbalanced device is due to uneven weight distribution of each blade attached to the rotor. Thus, any rotating element should be balanced, not only to minimize vibrations, but also to maximize the overall performance of the device. This overall performance may be interpreted as an increase in efficiency and reduction in fatigue of mechanical components. There are two major causes of failure for such a device. First, the device's acceleration could change with each revolution, thus causing loss of power with each rotation. Secondly, an unbalanced rotor produces unstable loads, which may cause fatigue failure on other mechanical components of the system.

Another aspect that it is recommended for future research is related to wind speeds. This entire project was developed assuming a wind speed of 32.5 m/s which corresponds to a category 1 hurricane. This is a very important component of the further development of this new idea because it will expand the range of operation of the turbine, which will ultimately save lives and economic resources.

Another very important aspect recommended to develop as a continuation of this project is a stress analysis. The scope of the present study did not include a stress analysis in the proposed design. Performing a stress analysis will allow the turbine to be built using more affordable materials while maintaining a safe operation. This will ultimately affect the end user who will be able to better afford such kind of device. Furthermore, a stress analysis will become even more important when higher wind speeds are considered. There

are already many products in the market that can withstand the wind speeds used for this project; nevertheless, higher wind speeds need more attention.

Another consideration that was disregarded for this project is the structural component on how to attach the device to the house. This team considers that it is more suited for a senior design team composed of civil engineers to analyze this matter. Civil engineers should be able to determine different ways in which the device can be attached to the house while maintaining aesthetic appeal. Furthermore, this civil engineering team could determine all the above mentioned aspects while following state and national construction codes and regulations, which represents the main reason for this team to appoint a civil engineering team as the best candidate for this particular component.

Another topic that was not studied in this project is the cornering wind vortices. This team recommends performing studies to determine if this device can also be used to mitigate these vortices because they are known to cause serious damage to houses during high speed winds.

One more recommendation that must be mentioned is related to a three dimensional analysis. Due to the lack of computing resources available to the team during the development of this project, only two dimensional simulations were performed. For future studies, a 3D analysis is recommended in order to obtain results that can be much closer to the real values. It is important to mention that, since this project represents the very first step in a completely new field of wind mitigation studies, a 2D analysis was sufficient to prove the objectives set at the beginning of this project. However, if a deeper analysis is to

be performed in the future, three dimensional simulations will yield much more accurate results.

Another subject for future studies to follow up this project is related to biphasic flows. In other words, the idea presented in this project could be further elaborated by performing a similar analysis using a mix of wind and water as the working fluid for the turbine. This could represent a very important addition to the present project because during hurricanes that is a very common mixture to which the device will be exposed to. Therefore, a biphasic fluid is as a recommendation for future studies to build upon the present thesis.

Finally, another idea that came across the team was to design a cover or curtain to the device. Due to limited time, this idea could not be developed and studied, and for that reason it becomes a recommendation as a follow up study. Such cover could be placed in front of the device to redirect the wind. If a complete and thorough study is performed on this subject, both the mitigation and power generation capabilities of the device could be significantly improved.

All the recommendations mentioned above will contribute to the development of a very efficient power-generating wind mitigation device with the ability to save lives.

11. REFERENCES

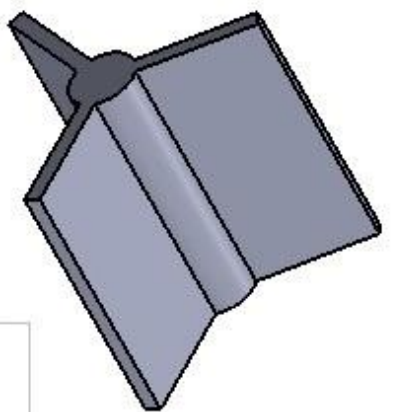
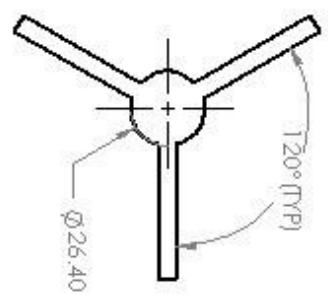
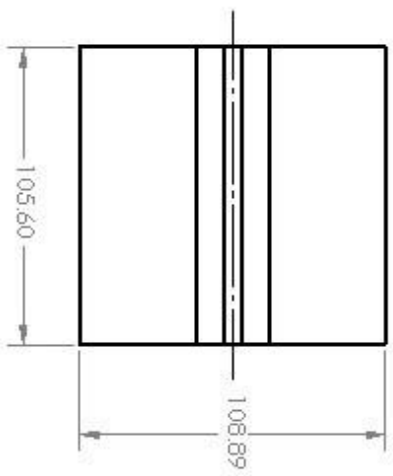
- (n.d.). Retrieved from Rooftop Mounted Vertical Axis Helix Wind Turbine Energy:
<http://helixturbineenergy.com/>
- Hirsch, R. L., Bezdek, R., & Wendling, R. (2005). Peaking of World Oil Production: Impacts, Mitigation & Risk Management. *Department of Energy*.
- Ali, M. H. (Sep - Oct. 2013). Experimental Comparison Study for Savonius Wind Turbine of Two & Three Blades At Low Wind Speed. *International Journal of Modern Engineering Research (IJMER)*, 2978-2986.
- American Society of Civil Engineers Online Library*. (n.d.). Retrieved from
<http://ascelibrary.org/>
- Beri, H., & Yao, Y. (2011). Double Multiple Stream Tube Model and Numerical Analysis of Vertical Axis Wind Turbine. *Scientific Research*. Retrieved from
<http://www.scirp.org/journal/PaperInformation.aspx?paperID=6380>
- Budynas, R., & Nisbett, K. (2011). *Shigley's Mechanical Engineering Design* (9th ed.). McGraww-Hill.
- Childs, P. R. (2011). *Rotating Flow*. Oxford: Butterworth-Heinemann.
- Electropaedia, Energy Sources and Energy Storage*. (n.d.). Retrieved from
http://www.mpoweruk.com/wind_power.htm
- Energy, U. D. (n.d.). *Office of Scientific & Technical Information*.
- Energy, U. D. (n.d.). Wind Energy Update. *National Renewable Energy Laboratory*. Retrieved from <http://www.windpoweringamerica.gov/>

- ESPEYRAC, L., & PASCAUD, S. (n.d.). *Strouhal Instability - Von Karman Vortex Street*. Retrieved January 24, 2014, from <http://hmf.enseeiht.fr>.
- ExxonMobil. (2014). *The Outlook for Energy: A View to 2040*.
- Goudarzi, N., & Zhu, W. (2013). A review on the development of wind turbine generators. *pringer-Verlag*, 11.
- Government, U. S. (2009). American Recovery and Reinvestment Act of 2009.
- Government, U. S. (n.d.). *Department of Energy*. Retrieved from <http://energy.gov/>
- Government, U. S. (n.d.). *National Hurricane Center*. Retrieved from <http://www.nhc.noaa.gov/>
- Government, U. (n.d.). *Window on State Government*. Retrieved from <http://www.window.state.tx.us/specialrpt/energy/renewable/wind.php>
- <http://ascelibrary.org/>. (n.d.). Retrieved October 26, 2013, from American Society of Civil Engineers Online Library.
- Kreith, F. (1999). *"Fluid Mechanics" Mechanical Engineering Handbook*. Boca Raton: CRC Press LLC.
- Lin, J., Montpellier, P., Tillman, C., & Riker, W. (2008). Aerodynamic Devices for Mitigation of Wind Damage Risk. *RenaissanceRe*. Retrieved from <http://www.renre.com/>
- Makerbot Website Faq*. (2014, March 30). Retrieved from Makerbot Website: <http://www.makerbot.com/faq/>
- Manwell, J., McGowan, J., & Rogers, A. (2009). *Wind Energy Explained: Theory, Design and Application* (2nd ed.). Wiley.

- MITOpenCourse. (2007). *MITOpenCourseWare*. Retrieved January 2014, from
Massachusetts Institute of Technology.
- Optimización Aerodinámica y Estructural de un Generador Eólico de Eje Vertical*. (n.d.).
Retrieved from Universidad Pontificia Bolivariana:
[http://kosmos.upb.edu.co/web/uploads/articulos/\(A\)_Optimizacion_Aerodinamica_y_Estructural_de_un_Generador_Eolico_de_Eje_Vertical_1097.pdf](http://kosmos.upb.edu.co/web/uploads/articulos/(A)_Optimizacion_Aerodinamica_y_Estructural_de_un_Generador_Eolico_de_Eje_Vertical_1097.pdf)
- Oy Windside Production Ltd*. (n.d.). Retrieved January 6, 2014
- Paraschivoiu, I. (2009). *Wind Turbine Design With Emphasis on Darrieus Concept* (1st ed.). Quebec: Press Internationale Polytechnique.
- Pritchard, P. J. (2011). *Fluid Mechanics*. Wiley.
- Ragheb, M. R. (2011). Wind Turbines Theory - The Betz Equation and Optimal Rotor Tip Speed Ratio. In D. R. Carriveau, *Fundamental and Advanced Topics in Wind Power*. Urbana: University of Illinois.
- RenaissanceRe*. (n.d.). Retrieved from <http://www.renre.com/>
- Sagrillo, M. (2002). Apples and Oranges, Choosing a Home-Sized Wind Generator. *Home Power*, 17. Retrieved January 2014, from Home Power.
- University, F. I. (n.d.). *Florida International University International Hurricane Research Center*.
- White, F. M. (2001). *Fluid Mechanics, Fourth Edition*. McGraw-Hill.
- Wind Turbine Industries Corp*. (n.d.). Retrieved January 2014

12. APPENDIX

12.1 Appendix A: Engineering Drawings



Note:
 • Remove sharp edges.

PROPRIETARY AND CONFIDENTIAL
 THE INFORMATION CONTAINED HEREIN IS THE PROPERTY OF THE DESIGNER AND IS NOT TO BE REPRODUCED OR TRANSMITTED IN ANY FORM OR BY ANY MEANS, ELECTRONIC OR MECHANICAL, INCLUDING PHOTOCOPYING, RECORDING, OR BY ANY INFORMATION STORAGE AND RETRIEVAL SYSTEM, WITHOUT THE WRITTEN PERMISSION OF THE DESIGNER.

UNLESS OTHERWISE SPECIFIED:		UNIT	DATE	REV
DIMENSIONS	AS SHOWN	MILLIMETERS	DD-21-12	
FINISHES	AS SHOWN			
CONCRETE				
STEEL				
WOOD				
GLASS				
PLASTER				
PAINT				
OTHER				
MATERIALS				
Plastic: PC				
OTHER MATERIALS				
DRAWN BY:				
CHECKED BY:				
DATE:				
SCALE:				
WEIGHT:				
SHEET 1 OF 1				

5 4 3 2 1

TITLE:
 Wind Turbine

SIZE: DWG. NO.
 A 3 Blades Variant1

SCALE: WEIGHT: SHEET 1 OF 1

